iScience

CellPress
OPEN ACCESS

Article

Experimental evolution of *Bacillus subtilis* on *Arabidopsis thaliana* roots reveals fast adaptation and improved root colonization

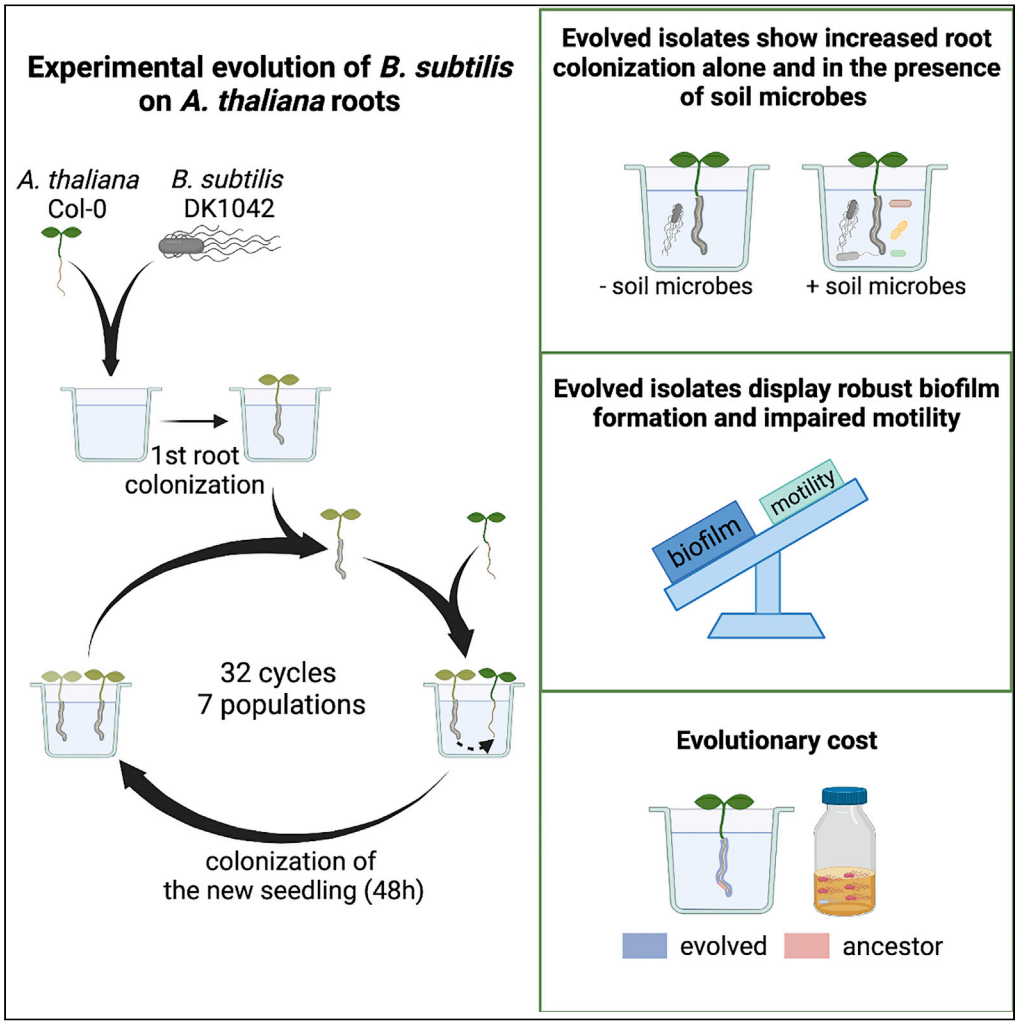

Mathilde Nordgaard, Christopher Blake, Gergely Maróti, Guohai Hu, Yue Wang, Mikael Lenz Strube, Ákos T. Kovács

atkovacs@dtu.dk

Highlights

Bacillus subtilis shows fast adaptation to *Arabidopsis thaliana* roots in a hydroponic setup

Evolved isolates exhibit robust biofilms in response to xylan and impaired motility

Adaptation to *A. thaliana* roots is accompanied by an evolutionary cost

An evolved isolate shows higher root colonization in the presence of soil bacteria

Nordgaard et al., iScience *25*, 104406
June 17, 2022
https://doi.org/10.1016/j.isci.2022.104406

iScience

CellPress
OPEN ACCESS

Article

Experimental evolution of *Bacillus subtilis* on *Arabidopsis thaliana* roots reveals fast adaptation and improved root colonization

Mathilde Nordgaard,[1] Christopher Blake,[1] Gergely Maróti,[2] Guohai Hu,[1,3] Yue Wang,[3,4] Mikael Lenz Strube,[5] and Ákos T. Kovács[1,6,*]

SUMMARY

***Bacillus subtilis* is known to promote plant growth and protect plants against disease. *B. subtilis* rapidly adapts to *Arabidopsis thaliana* root colonization, as evidenced by improved root colonizers already after 12 consecutive transfers between seedlings in a hydroponic setup. Re-sequencing of single evolved isolates and endpoint populations revealed mutations in genes related to different bacterial traits, in accordance with evolved isolates displaying increased root colonization associated with robust biofilm formation in response to the plant polysaccharide xylan and impaired motility. Interestingly, evolved isolates suffered a fitness disadvantage in a non-selective environment, demonstrating an evolutionary cost of adaptation to the plant root. Finally, increased root colonization by an evolved isolate was also demonstrated in the presence of resident soil microbes. Our findings highlight how a plant growth-promoting rhizobacterium rapidly adapts to an ecologically relevant environment and reveal evolutionary consequences that are fundamental to consider when evolving strains for biocontrol purposes.**

INTRODUCTION

The nutrient-rich rhizosphere is a hotspot for microbial activity, containing up to 10^{11} bacteria per gram root (Egamberdieva et al., 2008) and housing more than 30,000 prokaryotic species (Mendes et al., 2011). Among those are beneficial bacteria which are actively recruited by the plant through root exudate secretion and subsequently colonize the root from where they benefit the plant through various mechanisms (Berendsen et al., 2012, 2018; Mendes et al., 2011; Rudrappa et al., 2008; Trivedi et al., 2020). One well-known plant growth-promoting rhizobacterium (PGPR) is the spore-forming *B. subtilis* that has been isolated from various plant species (Cazorla et al., 2007; Fall et al., 2004; Huang et al., 2017; Pandey and Palni, 1997). Its plant-beneficial traits (Blake et al., 2021a) and promising role as a biocontrol agent (Fira et al., 2018; Kiesewalter et al., 2021; Ongena and Jacques, 2008) have fueled the interest in studying *B. subtilis*–plant interactions and led to the elucidation of mechanisms involved in the establishment of *B. subtilis* on the root and behind its plant beneficial properties.

An obvious prerequisite for successful root colonization is the ability of the bacterium to reach the plant root. Chemotaxis toward root exudates was shown to be important for the early colonization of *A. thaliana* roots by *B. subtilis* under hydroponic conditions (Allard-Massicotte et al., 2016), whereas solid surface motility has been suggested to play a role during tomato root colonization in vermiculites (Tian et al., 2021). After reaching the plant root, *B. subtilis* initiates biofilm formation (Allard-Massicotte et al., 2016; Bais et al., 2004; Beauregard et al., 2013; Chen et al., 2013). Similar to *in vitro* conditions, the formation of plant root-associated biofilms depends on the production of the matrix components EPS and TasA (Beauregard et al., 2013; Branda et al., 2006; Chen et al., 2013; Dragoš et al., 2018a). The expression of the operons involved in matrix production, *epsA-O* and *tapA-sipW-tasA*, is controlled by the biofilm repressor SinR (Chu et al., 2006; Kearns et al., 2005). In response to environmental cues, one or more of the five histidine kinases, KinA-E, are activated resulting in phosphorylation of the master regulator Spo0A through a phosphorelay (Jiang et al., 2000). At threshold concentrations of Spo0A ~ P, SinI is produced (Fujita et al., 2005), which binds to and inhibits SinR (Bai et al., 1993), resulting in matrix gene expression. As an environmental cue for root colonization, root exudates from tomatoes were shown to

[1]Bacterial Interactions and Evolution Group, DTU Bioengineering, Technical University of Denmark, 2800 Kongens Lyngby, Denmark

[2]Institute of Plant Biology, Biological Research Centre, Eötvös Loránd Research Network (ELKH), 6726 Szeged, Hungary

[3]China National GeneBank, BGI-Shenzhen, 518120 Shenzhen, China

[4]BGI-Beijing, BGI-Shenzhen, 100101 Beijing, China

[5]Bacterial Ecophysiology and Biotechnology Group, DTU Bioengineering, Technical University of Denmark, 2800 Kongens Lyngby, Denmark

[6]Lead contact

*Correspondence: atkovacs@dtu.dk

https://doi.org/10.1016/j.isci.2022.104406

trigger biofilm formation in *B. subtilis* in a KinD-dependent manner (Chen et al., 2012), whereas another study reported biofilm induction by plant polysaccharides via KinC and KinD (Beauregard et al., 2013). *B. subtilis* benefits from such microbe–plant interactions by acquiring carbon source from the plants. In turn, *B. subtilis* protects the plant against disease directly by producing antimicrobials (Asaka and Shoda, 1996; Bais et al., 2004; Chen et al., 2013; Kiesewalter et al., 2021) and indirectly through niche competition (Köhl et al., 2019; Lugtenberg and Kamilova, 2009) and elicitation of induced systemic resistance in the plant (Akram et al., 2015; Rudrappa et al., 2008). Moreover, *B. subtilis* promotes plant growth by improving nutrient availability and producing growth-promoting phytohormones (Blake et al., 2021a).

Mutualistic bacteria-plant interactions are a result of a long-term co-evolution of bacteria and plants that started with the colonization of land by ancestral plants 450 million years ago (Hassani et al., 2018). Here, we were interested in studying how *B. subtilis* adapts to plant roots on a much shorter evolutionary timescale. Experimental evolution (EE) provides a powerful tool to study microbial adaptation to different environments in real-time (Kawecki et al., 2012; Lenski, 2017). We recently studied EE of *B. subtilis* on *A. thaliana* plants roots, which revealed diversification of *B. subtilis* into three distinct morphotypes. A mix of the three morphotypes displayed increased root colonization compared with the sum of the three morphotypes in monocultures weighted by their initial relative abundance in the mix, which was demonstrated to be caused by complementarity effects (Blake et al., 2021b). Such morphological diversification has also been observed in EE of *B. subtilis* biofilm pellicles formed at the air-liquid interface (Dragoš et al., 2018b) as well as during EE of *Burkholderia cenocepacia* biofilms on polystyrene beads (Poltak and Cooper, 2011). In this study, we performed EE of *B. subtilis* on one-week-old *A. thaliana* roots under axenic conditions with the initial hypothesis that *B. subtilis* would adapt to the plant root environment by acquiring mutations that would provide the bacteria with a fitness advantage over the ancestor during root colonization. We found that *B. subtilis* rapidly adapted to the plant root as observed by improved root colonizers already after 12 consecutive transfers. In addition, two selected evolved isolates from independent populations from the final transfer (transfer 30) outcompeted the ancestor during root colonization. Furthermore, re-sequencing of single evolved isolates from independent populations and different time points as well as of the endpoint populations revealed mutations within (or upstream from) genes related to different bacterial traits. To further elucidate which bacterial traits were altered during the adaptation to plant roots, evolved isolates from the final transfer were subjected to additional phenotypic characterization. We found that evolved isolates from independent populations displayed robust biofilm formation in response to plant polysaccharides, impaired motility, and altered growth on plant compounds. Finally, we demonstrate that adaptation of *B. subtilis* to *A. thaliana* roots is accompanied by an evolutionary cost, and report an evolved isolate displaying increased root colonization also in the presence of resident soil microbes.

RESULTS

B. subtilis populations evolved on *A. thaliana* roots show a rapid increase in root colonization

To explore the evolutionary adaptation of *B. subtilis* to plant roots, we employed an experimental evolution (EE) setup previously established for another *Bacillus* species (Lin et al., 2021). In short, *B. subtilis* DK1042 (hereafter referred to as the ancestor) was inoculated onto *A. thaliana* seedlings under hydroponic conditions in seven parallel populations. The MSNg medium used in the EE is a minimal medium supplemented with a very low concentration of glycerol (0.05%), and the bacteria thereby move toward the plant root to access a carbon source. Every 48 h for a total of 64 days, the newly colonized seedling was transferred to a fresh medium containing a new sterile seedling, thereby enabling re-colonization (Figure 1A). We hypothesized, that during the successive transfers *B. subtilis* would adapt to the plant roots by acquiring mutations that would confer a fitness advantage over the ancestor during root colonization, resulting in these mutations being selected. In this setup, we specifically selected for a regular cycle of dispersal from the root-associated biofilm, chemotaxis toward the new root, and biofilm formation on the root surface. To follow potential changes in root colonization of the evolving populations during the ongoing EE, the productivity, i.e. colony-forming unit (CFU) per root, was quantified at different time points. All seven independent populations showed a rapid increase in root colonization within the first seven transfers, after which the productivity of the populations remained rather stable with slight increases and drops dependent on the certain population (Figure 1B). While this rapid increase in productivity could be owing to genetic adaptation to the plant root, the initial rise could also be caused by physiological adaptation to the experimental conditions. Interestingly, such a rapid increase in productivity of populations evolving on plant roots is consistent with our recent study where *B. subtilis* evolved on older *A. thaliana* roots (Blake et al., 2021b).

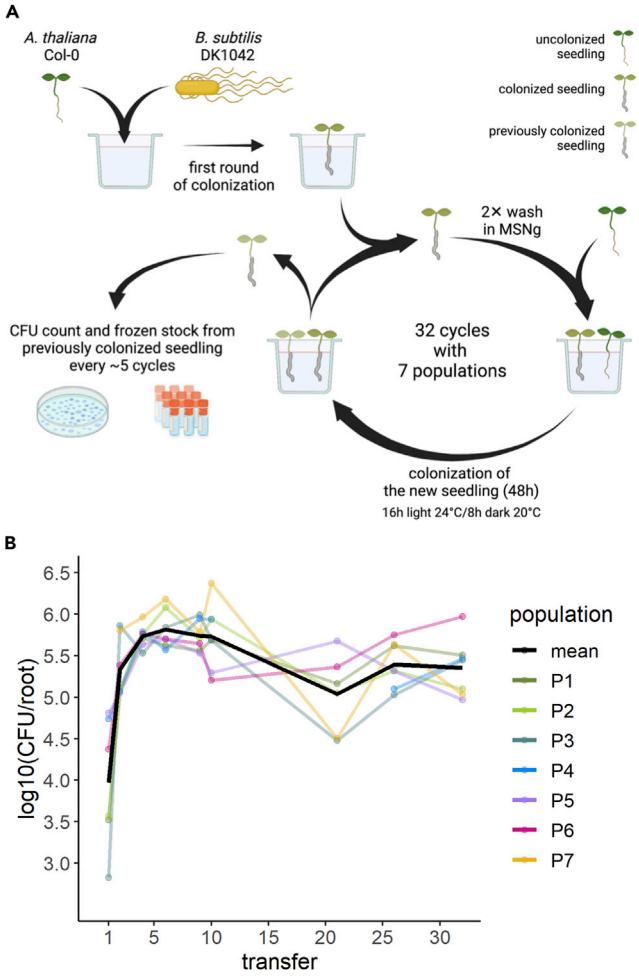

Figure 1. Overview of experimental evolution and productivity of evolving populations

(A) Overview of the experimental evolution approach. Created on BioRender.com.

(B) The *B. subtilis* populations rapidly increased in productivity during the experimental evolution on *A. thaliana* roots. The productivity (CFU/root) of the evolving populations was systematically quantified as CFU/root at nine different time points during the ongoing EE. The *y* axis displays the log10-transformed productivity. The black line represents the mean population productivity ($N = 7$).

Several evolved isolates display altered colony morphologies

To examine whether genetic adaptation to the plant root had taken place during the EE, single evolved isolates from the evolved populations were saved as frozen stocks and subjected to phenotypic and genotypic characterization. To represent different populations and time points during the EE, three isolates were randomly picked from each of population 3, 4, 6, and 7 at transfer 12, 18, and 30 (hereafter referred to as T12, T18, and T30). To detect possible changes in colony morphology, ON cultures of the ancestor and evolved isolates were spotted on LB agar and colonies inspected after 48-h incubation. On LB agar, the ancestor formed a round colony with a wrinkled periphery, whereas different colony morphologies were observed among the evolved isolates (Figure 2). At T12, some isolates displayed a colony morphology resembling the ancestor, e.g. isolate 3 from population 3 (3.3) and isolate 2 from population 7 (7.2), referred to as the "Wrinkled"-type. Several other isolates formed a colony with a white sharp edge along the wrinkled periphery (including isolates 3.2, 4.3, 6.1, and 7.3), hereafter referred to as the "Sharp-Wrinkled"-type. Additionally, isolate 7.1 formed a hyper-wrinkled, white colony, referred to as the "Snow"-type. These distinct colony morphologies were also observed at later time points (T18 and T30). Interestingly, the Snow-type was only observed in population 7. Furthermore, the three isolates from population 6 at T30 formed slightly less wrinkled colonies compared with the ancestor. We note that three isolates do not represent the entire population, and isolates with other colony morphologies could be present in

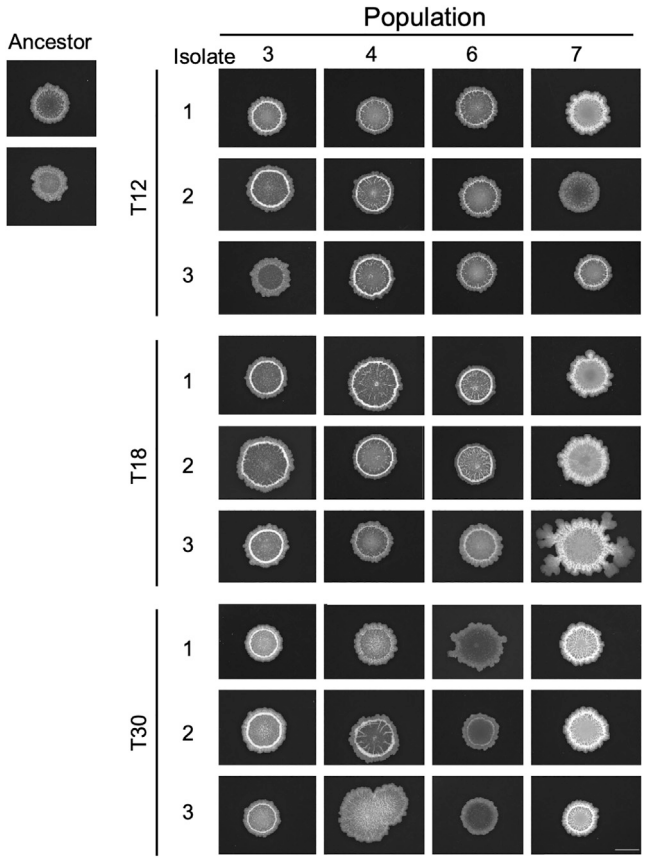

Figure 2. Distinct colony morphologies are observed among evolved isolates from different time points of the experimental evolution

ON cultures of the ancestor and evolved isolates from populations 3, 4, 6, and 7 at transfer 12, 18, and 30 were spotted on LB agar (1.5%) and imaged after incubation for 48 h at 30°C using a stereomicroscope. Ancestor represents *B. subtilis* DK1042. Each colony is representative of at least three replicates. Scale bar = 5 mm.

the populations. Nonetheless, the appearance of isolates with altered colony morphologies in the four populations indicates the presence of genetic changes. Furthermore, the occurrence of isolates with altered colony morphologies already at T12, and especially the presence of three different types (Wrinkled, Sharp-Wrinkled, and Snow) in population 7, at this early time point, suggests rapid diversification of *B. subtilis* during EE on *A. thaliana* roots. Such diversification into distinct morphotypes was also observed in our previous study on EE of *B. subtilis* on plant roots (Blake et al., 2021b) and has additionally been observed in EE of *B. subtilis* pellicle biofilms (Dragoš et al., 2018b), indicating successful adaptation to the selective environment.

Evolved isolates from different time points show increased colonization of *A. thaliana* roots

The design of the EE employed in this study should enable selection for bacteria that efficiently colonize the root. We, therefore, speculated whether the altered colony morphology of some of the evolved isolates was associated with improved productivity on the root (CFU/mm root). To test this, the ancestor and evolved isolates from the final time point (T30) were tested for individual colonization of *A. thaliana* seedlings under the same conditions applied during the EE. CFU quantification revealed that most evolved isolates tended to show increased root colonization, with five isolates from three different populations displaying significantly increased productivity on the root, with an up to circa 1.3-fold change relative to the ancestor (Figure 3). To track down when such improved root colonizers emerged during the EE, the randomly selected evolved isolates from T12 and T18 were similarly tested. Three and five evolved isolates at T12 and T18, respectively, displayed significantly increased productivity relative to the ancestor. In addition, a single isolate from T12 was significantly reduced in root colonization. These results confirm that

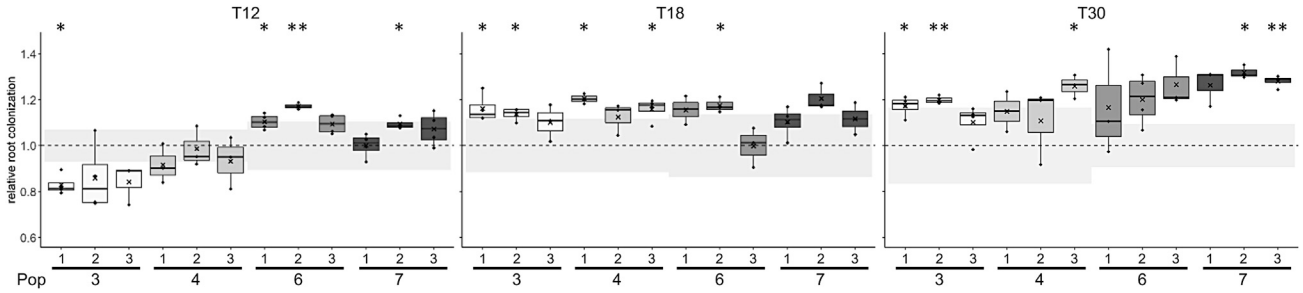

Figure 3. Evolved isolates from different time points show increased productivity on the root relative to the ancestor

The ancestor and evolved isolates from populations 3, 4, 6, and 7 at three different time points (T12, 18, 30) were tested for individual root colonization. For each evolved isolate, relative root colonization was calculated by dividing the log10-transformed productivity (CFU/mm root) of each replicate by the mean of the log10-transformed productivity of the ancestor from the same experimental setup. The cross represents the mean relative root colonization (N = 3-4). The dashed, horizontal line represents the mean of the ancestor (N = 3-4), whereas the grey-shaded rectangles represent the SD of the ancestor from the corresponding experiment. The normalized values were subjected to a One-sample t-test to test whether the mean was significantly different from 1. p-values have been corrected for multiple comparisons. *$p < 0.05$, **$p < 0.01$. See also Figure S2.

indeed the genetic adaptation of *B. subtilis* to the plant root took place during the EE. Furthermore, the observation of improved root colonizers already at T12 indicates that *B. subtilis* rapidly adapted to plant root colonization during the EE.

Selected evolved isolates display a fitness advantage over the ancestor that is specific to the plant root environment

While multiple evolved isolates displayed increased individual root colonization relative to the ancestor (Figure 3), we next wanted to test whether the evolved isolates had a noticeable fitness advantage over the ancestor during competition on the root. For this purpose, two selected evolved isolates from independent populations from T30 (Ev6.1 and Ev7.3, referring to isolate 1 from population 6 and isolate 3 from population 7, respectively) were competed against the ancestor on the plant root. Following 48 h of root colonization, CFU quantification revealed that both evolved isolates had outcompeted the ancestor on the root, and statistical analysis confirmed that the evolved isolates had a significantly higher fitness relative to the ancestor (Figure 4A; for calculation of relative fitness, see STAR Methods). This result was further supported by CLSM imaging: regardless of the fluorescence labeling combination, the two evolved isolates formed biofilms on the roots, as evidenced by aggregates along the root, whereas the ancestor was scarcely present (Figure 4C). Noticeably, the fluorescent images revealed that Ev6.1 formed fewer and smaller aggregates along the root compared with Ev7.3 (Figure 4C), consistent with the individual root colonization of the two isolates (Figure 3). To test whether the fitness advantage of Ev6.1 and Ev7.3 over the ancestor was specific to the plant root environment, the two evolved isolates competed against the ancestor in a non-selective environment, i.e. in LB supplemented with xylan, a plant polysaccharide (PP) found among others in the secondary cell walls of *A. thaliana* (Liepman et al., 2010), and under well-shaking conditions. In this non-selective environment, neither of the evolved isolates outcompeted the ancestor but instead seemed to suffer a fitness disadvantage compared with the ancestor, although the difference was statistically not significant (Figure 4B). Similar results were obtained for the permuted fluorescent combination (Figure S1). These results demonstrated that the evolved isolates had a fitness advantage over the ancestor specifically in the plant root environment. Furthermore, the loss of fitness in a different, non-selective environment suggests an evolutionary cost of adaptation to the plant roots (Bennett and Lenski, 2007; Elena and Lenski, 2003; van den Bergh et al., 2018).

Evolved isolates harbor mutations in genes related to different bacterial traits

To identify the genetic changes contributing to the increased root colonization (Figure 3) and fitness advantage over the ancestor during root colonization (Figures 4A and 4C), the genomes of selected evolved isolates were re-sequenced. To represent independent populations, the isolates from populations 6 and 7 at T30 were included. Furthermore, to track molecular evolution over time, the three isolates from population 7 at T12 and T18 were also re-sequenced. Finally, one isolate from population 1 (Ev1.1) at T30 was included for re-sequencing owing to its "Smooth" colony morphology and reduced root colonization (Figure S2). In the 13 re-sequenced isolates, we observed in total 51 unique mutations of which 37 were non-synonymous (Table S1). Isolate Ev1.1 harbored several mutations in *gtaB* encoding a UTP-glucose-1-phosphate

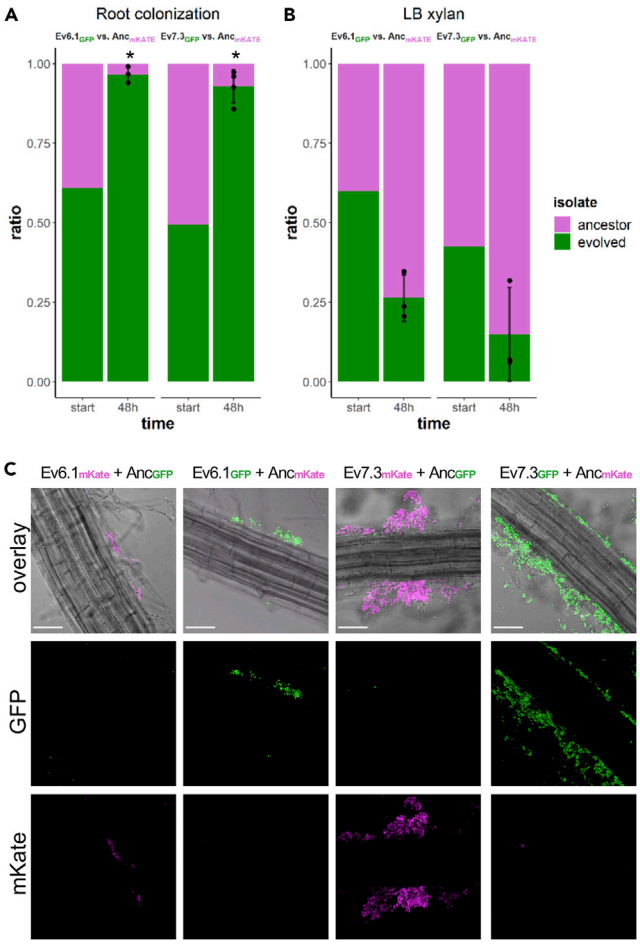

Figure 4. Two evolved isolates from transfer 30 outcompete the ancestor on the root but suffer a fitness disadvantage under shaking conditions in LB + xylan

(A and B) Pairwise competitions between ancestor (magenta) and evolved isolates (green) during root colonization (A) and in LB xylan (0.5%) under shaking conditions (B) for 48 h. In A and B, the bar plots show the starting ratio of the evolved isolate and ancestor in the mix, and the observed ratios after 48 h. Bars represent the mean (N = 3-4), the error bars represent the SD and the points show the replicates for the evolved (below) and ancestor (above). For statistical analysis, the relative fitness (r) of the evolved isolates was calculated by comparing the frequency of the evolved isolate at the beginning and end of the competition experiment. The log2-transformed relative fitness values were subjected to a One-sample t-test to test whether the mean was significantly different from 0. *$p < 0.05$.

(C) *A. thaliana* roots colonized by a 1:1 mix of ancestor and evolved isolates imaged by CLSM. Both fluorescence combinations are shown. The top row shows the overlay of the fluorescence channels and the bright field image. Images are representative of three independent *A. thaliana* seedlings. Color codes are shown at the top. Scale bar is 50 μm. See also Figure S1.

uridylyltransferase that synthesizes a nucleotide sugar precursor essential for the biosynthesis of exopolysaccharides (Varon et al., 1993) and for the synthesis of wall teichoic acids and lipoteichoic acid (Lazarevic et al., 2005). Two of the three isolates from population six at T30 (isolate Ev6.1 and Ev6.3) harbored a non-synonymous point mutation in the *fliM* gene, encoding a flagellar motor switch protein, part of the basal body C-ring controlling the direction of flagella rotation (Guttenplan et al., 2013). All three isolates in population 7 at T30 harbored a mutation in the intergenic region upstream from the *sinR* gene encoding a transcriptional repressor of the genes responsible for matrix production (Chu et al., 2006; Kearns et al., 2005). Interestingly, this mutation was also present in the three isolates in population 7 at T18 and in one of the isolates in this population at T12, suggesting that this mutation arose rather early in the EE and rose to a high frequency in population 7. Indeed, sequencing of the seven endpoint populations (i.e. the populations from T30) revealed that this mutation upstream from *sinR* was fixed in population 7 at the final time point, i.e. the mutation had reached a frequency of 1 in this population at T30 (Table S2). Furthermore, a

non-synonymous mutation within the *sinR* gene was detected at high frequencies in populations 2 and 3. In addition, non-synonymous mutations in genes related to flagellar motility were besides population 6 also observed in populations 3, 4, and 5 (*fliF*, *fliK*, *fliM*, and *hag*). Finally, mutations in genes related to cell wall metabolism (*gtaB*, *tagE*, and *walK*, encoded functions according to SubtiWiki (Zhu and Stülke, 2018)) were identified across all seven populations (Table S2). The detection of mutations within (or upstream from) genes related to biofilm formation, motility, and cell wall metabolism across independent populations supports the role of these mutations in the adaptation of *B. subtilis* to *A. thaliana* roots.

Evolved isolates show altered pellicle biofilm formation in response to plant polysaccharides

The fitness advantage of selected evolved isolates over the ancestor during root colonization (Figures 4A and 4C) and the detected mutations in the evolved isolates and endpoint populations (Tables S1 and S2) confirm our initial hypothesis, that *B. subtilis* adapted to the plant root by acquiring mutations that conferred a fitness advantage over the ancestor during root colonization.

Next, we wanted to elucidate which bacterial traits were altered during such adaptation to the plant root. For this purpose, evolved isolates from the final transfer (T30) were subjected to further phenotypic characterization. Given the detected mutations (Tables S1 and S2) and that both biofilm formation and motility are important for successful root colonization by *B. subtilis* (Allard-Massicotte et al., 2016; Beauregard et al., 2013; Chen et al., 2013; Tian et al., 2021), we hypothesized that these two bacterial traits would be under selection during the adaptation to the plant roots. To this end, plant polysaccharides (PPs) including xylan have been shown to induce biofilm formation in *B. subtilis* in a non-biofilm inducing medium (Beauregard et al., 2013). One way of adapting to the plant root could thereby be through enhanced biofilm formation in response to such PPs. To test whether the improved productivity on the root by the evolved isolates was associated with more robust biofilm formation in response to PPs, the ancestor and evolved isolates were tested for pellicle biofilm formation, a biofilm formed at the medium-air interface (Branda et al., 2001), in LB supplemented with xylan (LB + xylan). Importantly, a rich medium (LB) rather than the minimal medium (MSNg) was used in this assay to provide the bacteria with plenty of nutrients, allowing us to assess only the ability of the evolved isolates to form biofilm in response to xylan, and not the ability to utilize xylan for growth. We observed that a few isolates from T30 developed a pellicle biofilm similar to the ancestor, i.e. Ev4.1, Ev4.2, and Ev6.1 (Figure 5A). In contrast, the remaining isolates developed more robust pellicles with highly structured wrinkles indicative of enhanced matrix production. Especially the three isolates from population 7 developed hyper-robust, white pellicles, consistent with the Snow-type colony morphology observed for these isolates (Figure 2). The biofilms developed in response to xylan by the evolved isolates generally correlated with their productivity on the root. For example, isolates Ev4.1, Ev4.2, and Ev6.1 developing similar pellicles as the ancestor and isolates Ev7.1, Ev7.2, and Ev7.3 forming hyper-wrinkled, robust pellicles in response to xylan were among the ones showing the smallest and largest increase in individual root colonization (Figures 3 and 5A), respectively. This is in accordance with Chen et al. (2013) demonstrating that the ability of *B. subtilis* mutants to form robust biofilms *in vitro* correlated with that on the root. These results suggest that improved productivity on the root was associated with robust biofilm formation in response to xylan. To test whether this enhanced biofilm formation was specific to the presence of PPs, the ancestor and evolved isolates were tested for the ability to form pellicles in LB in the absence of xylan. In this medium, the pellicles developed by both the ancestor and evolved isolates were less robust (Figure S3). For most isolates, the improved biofilm formation was specific to the presence of PPs, whereas the isolates from population 7 displayed robust biofilms also in the absence of plant compounds suggesting a general improvement in biofilm formation in these isolates.

Evolved isolates show reduced swarming and swimming motility

To test whether the evolved isolates were affected in motility, the ancestor and evolved isolates from population 6 and 7 were tested for two types of motility: swimming motility, a single cell movement in aqueous environments powered by flagella rotation and swarming motility which is associated with a rapid multicellular movement of hyper-flagellated cells across a surface facilitated by self-produced surfactin (Kearns, 2010). Interestingly, most isolates were significantly impaired in both swimming and swarming motility (Figures 5B and 5C). Swimming motility was observed for the ancestor and evolved isolates after 4 h (Figure 5B). However, after 6 h only the ancestor and Ev6.2 had reached the edge of the Petri dish, whereas the remaining isolates reached at the most half of the swimming distance of the ancestor. Swarming was observed for the ancestor after 4 h which continued until the expanding colony almost reached the edge of the Petri dish after 8 h (Figure 5C). In contrast, the evolved isolates showed reduced or a complete

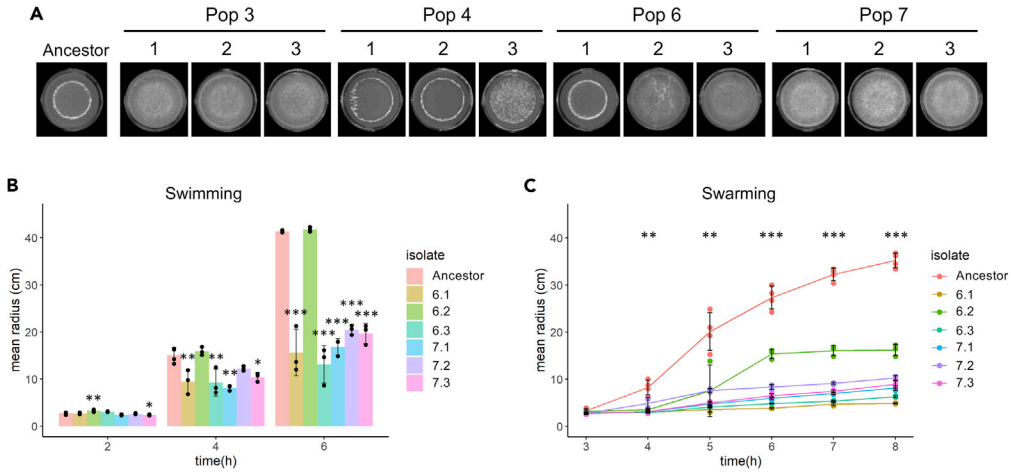

Figure 5. Evolved isolates from T30 show altered pellicle biofilm formation in response to plant polysaccharides and impaired motility

(A) Ancestor and evolved isolates from transfer 30 were inoculated into LB + 0.5% xylan at a starting OD_{600} of 0.05 in 24-well plates. Images were acquired after 48 h incubation at 30°C using a stereomicroscope. Each image is representative of four replicates. Each well has 16 mm width. Evolved isolates were tested for swimming (B) and swarming (C) motility in LB medium supplemented with 0.3 or 0.7% agar, respectively.

(B) Bars represent the mean (N = 3-4) and error bars represent SD.

(C) Lines represent the mean (N = 2-4) and error bars the SD. For the motility assays, the following statistical analysis applies: For each time point, an ANOVA was performed on the log10-transformed data followed by a Dunnett's Multiple Comparison test with the ancestor as the control. For swarming motility, the asterisks show the least significance observed for the given time point. At 3 h, only isolate 7.3 was significantly reduced in swarming motility. *$p < 0.05$, **$p < 0.01$, ***$p < 0.001$. See also Tables S1, S2, Figures S3, S4, and S5.

lack of swarming throughout the experiment. The evolution of motility-impaired isolates in independent populations could indicate that motility is not important for root colonization in the selective environment. Notably, during the EE the 48-well plates were continuously shaking at 90 rpm. We speculated, that these mildly shaking conditions could allow the bacteria to get into contact with the root by chance and thereby reducing the impact of motility on root colonization in the selective environment. To test whether motility is important during root colonization under shaking conditions, the ancestor (here referred to as "WT") was competed against a Δ*hag* mutant, deficient in the production of the flagellin protein, for three successive rounds of root colonization under static or shaking conditions (200 rpm). Under static conditions, the Δ*hag* mutant was significantly outcompeted by the WT (Figure S4). In contrast, under shaking conditions, the Δ*hag* mutant was able to co-colonize the root to similar levels as the WT. These results demonstrate that motility is important for competition on the root under static conditions but is not required under shaking conditions. Thereby, impaired motility of several of the evolved isolates is not expected to negatively influence the fitness of these isolates in the selective environment.

Evolved isolates show distinct growth profiles in a plant-mimicking environment

The minimal medium (MSNg) used in the EE should render the bacteria dependent on root exudates and dead plant material to survive. A simple way of adapting to this selective environment could be through the enhanced utilization of available plant compounds. To test this, we used a modified version of the minimal medium employed during the EE. Instead of 0.05% glycerol, the MSN medium was supplemented with 0.5% cellobiose (MSNc). Cellobiose is a disaccharide and a product of partial hydrolysis of cellulose, found in plant cell walls (Beauregard et al., 2013; Endler and Persson, 2011). In addition, MSNc was supplemented with 0.5% xylan. The ancestor showed a growth profile typical of bacterial growth under planktonic conditions (Figure S5). In contrast, several evolved isolates displayed distinct growth profiles, including 3.2, 7.1, 7.2, and 7.3, which showed no decline phase, but instead displayed a pro-longed stationary phase. When analyzing the carrying capacity (K), several isolates showed significantly increased carrying capacity (all three isolates from populations 3 and 7), whereas few isolates showed significantly decreased carrying capacity (Ev4.2, Ev4.3, and Ev6.2). While cellobiose and xylan do not completely represent the plant

compounds present in the selective environment, these results suggest that adaptation to the plant root could also be facilitated through the altered utilization of plant compounds.

An evolved isolate shows increased colonization of *A. thaliana* roots in the presence of a synthetic, soil-derived community

During the EE, *B. subtilis* was adapted to the plant root alone – in the absence of other microbes. This selective environment is far from its natural habitat in the rhizosphere, where *B. subtilis* encounters other microbial residents. In fact, the ancestor DK1042 is a derivate of the wild strain NCIB 3610, originally isolated from hay infusion (Cohn, 1930; Zeigler et al., 2008). To this end, we wondered how the pro-longed adaptation of *B. subtilis* to the plant root environment in the absence of other microbial species affected the ability to colonize the root in the presence of soil microbes. The ancestor and Ev7.3 were tested for their ability to colonize *A. thaliana* roots in the presence of a synthetic, soil-derived community (Lozano-Andrade et al., 2021). This community comprises four bacterial species, *Pedobacter* sp., *Rhodococcus globerulus*, *Stenotrophomas indicatrix* and *Chryseobacterium* sp. that were previously isolated from soil samples that also contained *B. subtilis*, thereby representing bacterial soil inhabitants that *B. subtilis* would normally encounter in nature. The isolate Ev7.3 was chosen for this test since it was highly adapted to the selective environment, i.e. the isolate displayed significantly increased individual root colonization (Figure 3) and outcompeted the ancestor during competition on the root, where it formed a robust biofilm along the root (Figures 4A and 4C). To capture any potential difference in the establishment on the root, here defined as root colonization after 48 h, between *B. subtilis* ancestor and Ev7.3 in the presence of the community, the ancestor or Ev7.3 was co-inoculated with the community in four different ratios: 0.1:1, 1:1, 10.1, and 100:1 of *B. subtilis* and community, respectively. When *B. subtilis* was initially under-represented or highly in excess, i.e. inoculation ratio 0.1:1 and 100:1, respectively, no significant difference was observed in the establishment on the root between *B. subtilis* ancestor and Ev7.3 within the same inoculation ratio (Figure 6). In contrast, when co-inoculated with the community in intermediate ratios, i.e. 1:1 and 10:1, isolate Ev7.3 showed significantly enhanced establishment on the root compared with the ancestor. Since Ev7.3 displayed increased carrying capacity in MSNc + xylan in monoculture compared with the ancestor (Figure S5), we wondered whether the enhanced establishment on the root by Ev7.3 in the presence of the community could be partly attributed to improved utilization of plant compounds. Indeed, growth profiles in MSNc + xylan of the ancestor or Ev7.3 in co-culture with the community revealed that Ev7.3 displayed a significantly increased carrying capacity at inoculation ratio 1:1, 10:1, and 100:1 compared with the ancestor (Figure S6). Finally, *in vitro* confrontation assays on LB agar (1.5%) showed no major difference in the inhibition of the community members by Ev7.3 compared with the ancestor (Figure S7). Taken together, these results show that even though *B. subtilis* was adapted to the plant root alone, isolate Ev7.3 displayed increased root colonization also in the presence of a synthetic, soil-derived community under certain inoculation ratios, possibly mediated by robust biofilm formation on the root and enhanced utilization of plant compounds.

DISCUSSION

Several studies have reported experimental evolution as a powerful tool to explore how bacteria adapt to ecologically relevant environments. A recent study investigated the adaptive response of the PGPR *Pseudomonas protegens* to the *A. thaliana* rhizosphere in a sand system, which revealed mutations in genes encoding global regulators and genes related to motility and cell surface structure across independent populations (Li et al., 2021b) and during such adaptation, the initially plant-antagonistic *P. protegens* bacterium evolved into mutualists (Li et al., 2021a). Furthermore, Lin et al. (2021) observed that adaptation of *Bacillus thuringiensis* to *A. thaliana* roots under hydroponic conditions led to the evolution of multicellular aggregating phenotypes, which, surprisingly, in certain lineages were accompanied by enhanced virulence against the *Galleria mellonella* larvae. Here, we employed experimental evolution to study the adaptation of *B. subtilis* to *A. thaliana* roots under hydroponic conditions. Our initial hypothesis was that *B. subtilis* would adapt to the plant roots by acquiring mutations that would provide the bacteria with a fitness advantage over the ancestor during root colonization. We could demonstrate that *B. subtilis* rapidly adapted to the plant roots, as observed by evolved isolates displaying improved root colonization relative to the ancestor already after 12 transfers and the detection of genetic changes in evolved isolates from transfer 12, 18, and 30. In addition, competition between the ancestor and two selected evolved isolates from the final transfer (T30) on the root revealed that both evolved isolates had a fitness advantage over the ancestor during root colonization, thereby confirming our hypothesis.

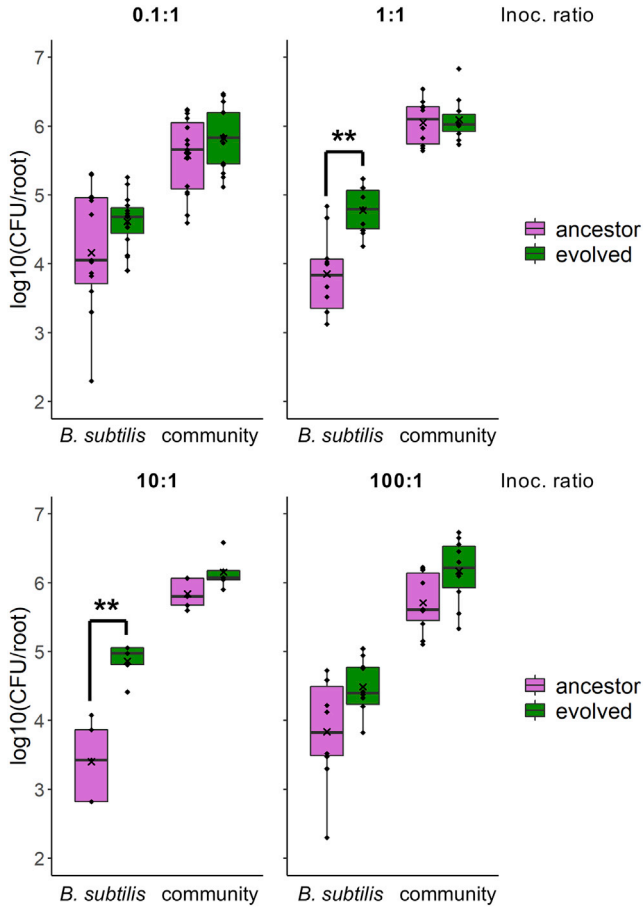

Figure 6. Root colonization by *B. subtilis* ancestor and isolate Ev7.3 in the presence of a synthetic, soil-derived community

The ancestor and evolved isolate, Ev7.3, were tested for the ability to colonize the root in the presence of a synthetic, soil-derived bacterial community. *B. subtilis* ancestor or Ev7.3 and the community were co-inoculated onto *A. thaliana* roots in four different ratios: 0.1:1, 1:1, 10:1, and 100:1 of *B. subtilis* and community, respectively. Root colonization after 48 h was quantified as log10-transformed productivity (CFU/root). Each plot shows the resulting root colonization at the given inoculation ratio of *B. subtilis* (left) and the co-inoculated community (right). Magenta: Ancestor and the corresponding community co-inoculated with the ancestor. Green: Ev7.3 and the community co-inoculated with Ev7.3. The cross represents the mean (N = 5–15). Within each inoculation ratio, statistical significance between *B. subtilis* ancestor and Ev7.3, and between the communities co-inoculated with the ancestor or with Ev7.3 was tested with a Two-sample t-test (Welch's Two-sample t-test when unequal variance). **$p < 0.01$. See also Figures S6 and S7.

Further phenotypic characterization of the evolved isolates from the final transfer revealed that most isolates across independent populations developed more robust biofilms in response to the plant polysaccharide xylan compared with the ancestor. Except for isolate Ev3.3, the robust biofilm formers tended to be increased in individual root colonization, indicating that robust biofilm formation is associated with adaptation to the plant root. Motility represents an important trait for many bacteria as it allows them to explore the environment for nutrients and escape unfavorable conditions. Of relevance to the adaptation of *B. subtilis* to plant roots, motility has been shown to be important for root colonization of different plant species under different conditions. For example, a *B. subtilis* Δ*hag* mutant was shown to be delayed or reduced in *A. thaliana* root colonization under hydroponic conditions as well as in tomato root colonization under vermiculites pot conditions (Allard-Massicotte et al., 2016; Tian et al., 2021). Yet, we found that five out of six isolates from two independent populations were impaired in both swimming and swarming motility, indicating that motility is not important for root colonization in the selective environment of the EE, i.e. under hydroponic, shaking conditions. Indeed, this was verified in a competition experiment between a non-motile Δ*hag* mutant and the WT, revealing that motility is not required for root colonization under shaking conditions. In contrast to our observations, Li et al. (2021a) observed several evolved isolates

of *P. protegens* improved in swimming motility following adaptation to the *A. thaliana* rhizosphere in a sand system (Li et al., 2021b), supporting that in sand (and thus possibly also in soil), motility is indeed important for root colonization and is therefore selected for.

In *B. subtilis*, motility and biofilm formation are incompatible processes: *B. subtilis* can exist as single, motile cells or in chains of sessile, matrix-producing cells which is regulated by an epigenetic switch involving SinR (Chai et al., 2010; Vlamakis et al., 2008). The enhanced biofilm formation and impaired motility of isolates from populations 6 and 7 (Ev6.3, Ev7.1, Ev7.2, and Ev7.3) could thereby indicate a possible biofilm-motility trade-off. An inverse evolutionary trade-off between biofilm formation and motility was observed when the opportunistic pathogen *Pseudomonas aeruginosa* was subjected to repeated rounds of swarming that lead to the evolution of hyper-swarmers that were impaired in biofilm formation (van Ditmarsch et al., 2013). Considering that the ability to form robust biofilm *in vitro* was shown to positively correlate with root colonization in *B. subtilis* (Chen et al., 2013), and the demonstration that motility is not important for root colonization under shaking conditions, a possible biofilm-motility trade-off could provide *B. subtilis* with enhanced fitness during root colonization in the selective environment. Indeed, isolate Ev7.3, which developed hyper-robust biofilms in LB + xylan and was impaired in motility, significantly outcompeted the ancestor during root colonization.

Re-sequencing of selected evolved isolates revealed that Ev7.1, Ev7.2, and Ev7.3 (from transfer 30) all harbored a single nucleotide polymorphism (SNP) two base pairs upstream from the start codon of the *sinR* gene (Agarwala et al., 2018), encoding a transcriptional repressor of matrix genes (Chu et al., 2006; Kearns et al., 2005). This SNP is located in the spacer region between the Shine Dalgarno sequence and the start codon in the ribosome binding site. Interestingly, the nucleotide composition of the spacer sequence has been shown to influence translation efficiency (Liebeton et al., 2014). The SNP upstream from *sinR* might thereby potentially affect the translation efficiency from the mRNA transcript, resulting in reduced levels of SinR. Reduced levels of SinR could in turn result in increased expression of matrix genes. This is supported by Richter et al. (2018) who demonstrated that a Δ*sinR* mutant shows increased matrix gene expression, and by Subramaniam et al. (2013) reporting that SinR translation and therefore protein level affects matrix gene expression. Potential increased matrix production caused by this mutation could contribute to the Snow-type colony morphology, as this colony morphology was exclusively observed for isolates harboring this mutation. Furthermore, in accordance with the robust biofilm formation and increased root colonization observed for Ev7.1, Ev7.2 and Ev7.3, a Δ*sinR* mutant was shown to form a hyper-robust biofilm in biofilm-inducing medium as well as on tomato roots (Chen et al., 2013), supporting the possible relevance of this mutation for the observed phenotypes of these isolates. Based on these previous studies, we therefore speculate that the mutation upstream from *sinR* results in increased matrix gene expression, which in turn enables more robust biofilm formation and increased root colonization as observed for the three isolates in population 7. These three isolates did not harbor mutations in motility-related genes. However, besides a possible effect of reduced SinR levels on the epigenetic switch (Chai et al., 2010) that could lock the cells in a sessile, matrix-producing stage, a potential reduction in SinR levels leading to overexpression of the *eps* operon could possibly reduce motility owing to the EpsE clutch (Blair et al., 2008). Such mutation and the observed corresponding phenotypes could be responsible for the biofilm-motility trade-off, and be an example of antagonistic pleiotropy (Elena and Lenski, 2003) in which the same mutation is beneficial in one environment, i.e. during root colonization under shaking conditions, but disadvantageous in another, i.e. where motility is required for survival. In addition, this mutation affecting a biofilm regulator could possibly explain why Ev7.1, Ev7.2, and Ev7.3 show improved biofilm formation also in the absence of xylan.

Isolate Ev6.1 and Ev6.3 harbored a non-synonymous point mutation in the *fliM* gene, which was not present in Ev6.2. This gene encodes a flagellar motor switch protein, part of the basal body C-ring controlling the direction of flagella rotation (Guttenplan et al., 2013). Interestingly, Ev6.1 and Ev6.3 were impaired in both forms of motility, whereas Ev6.2 showed similar swimming as the ancestor and was less affected in swarming. We speculate that the R326I substitution affects the function of FliM and consequently the flagellar machinery, resulting in hampered motility in these two isolates. Since we showed that motility was not important for root colonization under shaking conditions, a mutation hampering motility could provide the bacterium a fitness advantage during the adaptation to *A. thaliana* roots owing to the reduced cost of this apparently redundant trait. However, we do not expect the mutation in *fliM* to result in reduced cost; it merely changes an amino acid in a protein part of the flagellar machinery. Other mutations in the population six isolates must explain the robust biofilm formation by Ev6.2 and Ev6.3 and the

fitness advantage of Ev6.1 over the ancestor during root colonization. For example, isolate Ev6.1 and Ev6.3 harbor a mutation in *kinA* encoding a two-component sensor kinase which once activated initiates the phosphorelay leading to phosphorylation of the master regulator Spo0A (Jiang et al., 2000).

The isolate from population one at transfer 30 (Ev1.1) harbored a frameshift mutation in the *rsiX* locus, encoding an anti-sigma factor controlling the activity of SigX (Zhu and Stülke, 2018). Inconsistent with the smooth morphology and reduced root colonization of this isolate, an Δ*rsiX* mutant was shown to have increased *eps* expression (Martin et al., 2020). However, Ev1.1 additionally harbored several mutations in *gtaB* encoding a UTP-glucose-1-phosphate uridylyltransferase involved in the biosynthesis of a nucleotide sugar precursor for EPS biosynthesis (Varon et al., 1993). A study conducted by Reverdy et al. (2018) showed that acetylation of GtaB is important for biofilm formation of *B. subtilis* and that a *gtaB* mutant was reduced in pellicle formation. In addition, Xu et al. (2019) showed that a Δ*gtaB* mutant of *Bacillus velezensis* SQR9 was significantly decreased in colonization of cucumber roots compared with the WT, although the effect of *gtaB* on root colonization may be species-dependent. We therefore speculate that Ev1.1 may have first gained the mutation in *rsiX* and was selected for owing to increased *eps* expression, whereas later on the increased matrix production was reverted by the mutations in *gtaB*, resulting in a non-functional protein and thereby reduced precursors for EPS production, which was selected for owing to the reduced cost. In accordance with the mutations observed in this study, a non-synonymous mutation in *sinR* in two isolates forming Snow-type colonies and increased in root colonization as well as several mutations in *gtaB* in two isolates with a Smooth colony morphology were observed in our recent study on diversification of *B. subtilis* during adaptation to *A. thaliana* roots (Blake et al., 2021b).

To get a more general insight into the mutations arising in *B. subtilis* during EE on *A. thaliana* roots, the seven endpoint populations were also sequenced. This revealed mutations within (or upstream from) genes related to biofilm formation (*sinR*), flagellar motility (*fliF*, *fliK*, *fliM*, and *hag*), and cell wall metabolism (*gtaB*, *tagE*, and *walK*) (Zhu and Stülke, 2018) across independent populations. Taken together, our findings of evolved isolates displaying altered biofilm formation and motility properties and the detection of mutations within (or upstream from) genes related to biofilm formation and motility in single evolved isolates as well as across independent endpoint populations indicates that adaptation of *B. subtilis* to *A. thaliana* roots under the employed conditions is associated with alterations in these two bacterial traits.

While we found that the phenotypic and genetic changes of Ev6.1 and Ev7.3 conferred a fitness advantage over the ancestor during root colonization, adaptation to one certain environment may be accompanied by a loss of fitness in other environments (Elena and Lenski, 2003). This has been demonstrated for *Escherichia coli* which following adaptation to low temperature showed reduced fitness at high temperature (Bennett and Lenski, 2007). In the example of the evolution of hyper-swarmers of *P. aeruginosa*, the hyperswarmer clones outcompeted the ancestor in swarming, but lost in biofilm competitions (van Ditmarsch et al., 2013). In this study, we demonstrate that adaptation of *B. subtilis* to *A. thaliana* roots is accompanied by an evolutionary cost. When Ev6.1 and Ev7.3 each were competed against the ancestor in LB + xylan under shaking conditions, i.e. an environment where plant compounds are present but biofilm formation is not required for survival, both evolved isolates suffered a fitness disadvantage. The observation that two evolved isolates, from independent populations and with different phenotypes and genetic changes, both suffered a fitness disadvantage in a non-selective environment might suggest the generality of such an evolutionary cost accompanying adaptation to *A. thaliana* roots.

In our EE approach, *B. subtilis* was adapted to plant roots in the absence of other microbes. In the rhizosphere environment under natural conditions, *B. subtilis* is far from being the sole microbial inhabitant. Instead, it engages in cooperative and competitive interactions with other members of the rhizosphere microbiome (Hassani et al., 2018; Kiesewalter et al., 2021). We tested whether the evolved isolate, Ev7.3, displaying increased root colonization in the selective environment relative to the ancestor, would also show improved establishment on the root under more ecologically complex conditions. We found that in the presence of a synthetic, soil-derived community, Ev7.3 displayed enhanced establishment on the root compared with the ancestor in two out of four inoculation ratios. This enhanced establishment on the root by Ev7.3 is not expected to be caused by altered antagonistic activities toward the community members. First, no major changes in the inhibition of the community members were observed in confrontation colony assays. Secondly, an increased number of Ev7.3 cells on the root did not cause a reduction in the co-colonizing community. Finally, Ev7.3 did not harbor mutations in genes directly related to secondary metabolite production. Instead, enhanced establishment on the root by Ev7.3 in the presence of the

community is possibly enabled by robust biofilm formation facilitating stronger attachment to the root and enhanced utilization of plant compounds. Interestingly, a study by Molina-Santiago et al. (2019) showed that compared with a Δmatrix mutant, co-inoculation of *B. subtilis* WT with *Pseudomonas chlororaphis* on melon leaves enabled co-localization of the two species as well as the closer attachment of *B. subtilis* to the left surface (Molina-Santiago et al., 2019). The robust biofilm formed on the root by Ev7.3 possibly facilitated by increased matrix production may thereby not exclude the community members on the root but could rather allow them to incorporate into the matrix. This could also explain why the enhanced establishment of *B. subtilis* Ev7.3 on the root did not cause a reduction in the number of community cells attached to the root. Alternatively, the community may not be majorly affected by any difference in the establishment on the root between the ancestor and Ev7.3 owing to the low abundance of *B. subtilis* relative to the community. Further work is needed to elucidate the interactions between *B. subtilis* and this synthetic community during root colonization. In summary, these findings suggest that even though *B. subtilis* was evolved on *A. thaliana* in the absence of other microbes, it became highly adapted to the plant root environment enabling better establishment on the root also when the ecological complexity increases. How genetic adaptation to the plant root in the absence of other microbial species differs from adaptation to plant root environments with varying levels of ecological complexity is the scope of future studies.

The formation of root-associated biofilms is important for the biocontrol efficacy of *B. subtilis* (Chen et al., 2013). From an applied perspective, experimental evolution of *B. subtilis* on plant roots represents an unexplored approach for developing strains with improved root attachment abilities for agricultural use. However, a biofilm-motility tradeoff as observed here may be undesirable when developing biocontrol agents owing to the growing evidence of motility as an important trait for bacterial root colonization in soil systems (Li et al., 2021b; Tian et al., 2021). The phenotypes associated with the adaptation of *B. subtilis* to *A. thaliana* roots presented here as well as the accompanying evolutionary cost and the increased root colonization also in the presence of resident soil bacteria highlight the importance of considering the selective environment if evolving PGPR for biocontrol purposes.

Limitations of the study

This study on the evolutionary adaptation of *B. subtilis* to *A. thaliana* roots under hydroponic conditions revealed that *B. subtilis* rapidly adapted to the plant root environment as observed by improved root colonizers already after 12 transfers. Moreover, we found that one selected evolved isolate displayed increased root colonization also in the presence of resident soil bacteria. The findings from this study thereby highlight experimental evolution as an approach to developing *B. subtilis* strains with improved root colonization capacities to potentially support a sustainable agricultural production. However, such plant root adaptation might be condition-specific, and we do not know whether the evolved isolates also display increased root colonization under soil conditions reminiscent of those the bacteria will encounter under greenhouse or field conditions. To this end, motility has been shown to be important for root colonization under diverse conditions, including soil and sand conditions (Gao et al., 2016; Tian et al., 2021). Thereby, the biofilm-motility trade-off observed for several of the evolved isolates might be undesirable in a biocontrol strain used under field or greenhouse conditions. Future studies will therefore test the evolved isolates for root colonization under greenhouse soil conditions to reveal whether adaptation to plant roots under the simple axenic, hydroponic conditions employed in this study, manifests in increased root colonization also under agriculturally relevant conditions.

STAR★METHODS

Detailed methods are provided in the online version of this paper and include the following:

- KEY RESOURCES TABLE
- RESOURCE AVAILABILITY
  - Lead contact
  - Materials availability
  - Data and code availability
- EXPERIMENTAL MODEL AND SUBJECT DETAILS
  - Bacterial strains and culture media
  - Plant material
- METHOD DETAILS

- Experimental evolution of *B. subtilis* on *A. thaliana* seedlings
- Isolation of single evolved isolates and colony morphology assay
- Root colonization assay
- Pairwise competition experiments in LB + xylan
- Biofilm formation in response to plant polysaccharides
- Motility assays
- Growth in the presence of xylan
- Pairwise interactions of *B. subtilis* with community members
- Microscopy/confocal laser scanning microscopy (CLSM)
- Genome re-sequencing and genome analysis of single isolates and endpoint populations

- QUANTIFICATION AND STATISTICAL ANALYSIS
  - Data and statistical analysis

SUPPLEMENTAL INFORMATION

Supplemental information can be found online at https://doi.org/10.1016/j.isci.2022.104406.

ACKNOWLEDGMENTS

We thank Carlos N. Lozano-Andrade for the four bacterial species constituting the synthetic community. The work was supported by a DTU Bioengineering start-up fund to ÁTK. Fundings from Novo Nordisk Foundation for the infrastructure "Imaging Microbial Language in Biocontrol (IMLiB)" (NNFOC0055625), and within the INTERACT project of the Collaborative Crop Resiliency Program (NNF19SA0059360) are acknowledged. The position of M.L.S. is financed by the Danish National Research Foundation (DNRF137) for the Center for Microbial Secondary Metabolites. G.H. and Y.W. were supported by China National GeneBank (CNGB).

AUTHOR CONTRIBUTIONS

Conceptualization, M.N.C., Á.T.K.; investigation, M.N.C., C.B.; formal analysis, M.N.C., M.L.S, G.M., G.H.; resources, G.M., G.H., Y.W.; writing – original draft, M.N.C., Á.T.K.; writing – review and editing, G.H., Y.W., G.M., M.L.S.; supervision, Á.T.K.; funding acquisition, Á.T.K.

DECLARATION OF INTERESTS

The authors declare no competing interests.

Received: August 10, 2021
Revised: January 22, 2022
Accepted: May 5, 2022
Published: June 17, 2022

REFERENCES

Agarwala, R., Barrett, T., Beck, J., Benson, D.A., Bollin, C., Bolton, E., Bourexis, D., Brister, J.R., Bryant, S.H., Canese, K., et al. (2018). Database resources of the National center for biotechnology information. Nucleic Acids Res. *46*, D8–D13. https://doi.org/10.1093/nar/gkx1095.

Akram, W., Anjum, T., and Ali, B. (2015). Searching ISR determinant/s from *Bacillus subtilis* IAGS174 against *Fusarium* wilt of tomato. BioControl *60*, 271–280. https://doi.org/10.1007/s10526-014-9636-1.

Allard-Massicotte, R., Tessier, L., Lécuyer, F., Lakshmanan, V., Lucier, J.F., Garneau, D., Caudwell, L., Vlamakis, H., Bais, H.P., and Beauregard, P.B. (2016). *Bacillus subtilis* early colonization of *Arabidopsis thaliana* roots involves multiple chemotaxis receptors. MBio *7*, e01664-16. https://doi.org/10.1128/mBio.01664-16.

Asaka, O., and Shoda, M. (1996). Biocontrol of *Rhizoctonia solani* damping-off of tomato with *Bacillus subtilis* RB14. Appl. Environ. Microbiol. *62*, 4081–4085. https://doi.org/10.1128/aem.62.11.4081-4085.1996.

Bai, U., Mandic-Mulec, I., and Smith, I. (1993). SinI modulates the activity of SinR, a developmental switch protein of *Bacillus subtilis*, by protein-protein interaction. Genes Dev. *7*, 139–148. https://doi.org/10.1101/gad.7.1.139.

Bais, H.P., Fall, R., and Vivanco, J.M. (2004). Biocontrol of *Bacillus subtilis* against infection of Arabidopsis roots by *Pseudomonas syringae* is facilitated by biofilm formation and surfactin production. Plant Physiol. *134*, 307–319. https://doi.org/10.1104/pp.103.028712.

Beauregard, P.B., Chai, Y., Vlamakis, H., Losick, R., and Kolter, R. (2013). *Bacillus subtilis* biofilm induction by plant polysaccharides. Proc. Natl. Acad. Sci. U. S. A. *110*, E1621–E1630. https://doi.org/10.1073/pnas.1218984110.

Bennett, A.F., and Lenski, R.E. (2007). An experimental test of evolutionary trade-offs during temperature adaptation. Proc. Natl. Acad. Sci. U S A. *104*, 8649–8654. https://doi.org/10.17226/11790.

Berendsen, R.L., Pieterse, C.M.J., and Bakker, P.A.H.M. (2012). The rhizosphere microbiome and plant health. Trends Plant Sci. *17*, 478–486. https://doi.org/10.1016/j.tplants.2012.04.001.

Berendsen, R.L., Vismans, G., Yu, K., Song, Y., De Jonge, R., Burgman, W.P., Burmølle, M., Herschend, J., Bakker, P.A.H.M., and Pieterse, C.M.J. (2018). Disease-induced assemblage of a plant-beneficial bacterial consortium. ISME J. *12*, 1496–1507. https://doi.org/10.1038/s41396-018-0093-1.

Blair, K.M., Turner, L., Winkelman, J.T., Berg, H.C., and Kearns, D.B. (2008). A molecular clutch disables flagella in the *Bacillus subtilis* biofilm. Science *320*, 1636–1638. https://doi.org/10.1126/science.1157877.

Blake, C., Christensen, M.N., and Kovács, Á.T. (2021a). Molecular aspects of plant growth promotion and protection by *Bacillus subtilis*. Mol. Plant Microbe Interact. *34*, 15–25. https://doi.org/10.1094/MPMI-08-20-0225-CR.

Blake, C., Nordgaard, M., Maróti, G., and Kovács, Á.T. (2021b). Diversification of *Bacillus subtilis* during experimental evolution on *Arabidopsis thaliana* and the complementarity in root colonization of evolved subpopulations. Environ. Microbiol. *23*, 6122–6136. https://doi.org/10.1111/1462-2920.15680.

Branda, S.S., Chu, F., Kearns, D.B., Losick, R., and Kolter, R. (2006). A major protein component of the *Bacillus subtilis* biofilm matrix. Mol. Microbiol. *59*, 1229–1238. https://doi.org/10.1111/j.1365-2958.2005.05020.x.

Branda, S.S., González-Pastor, J.E., Ben-Yehuda, S., Losick, R., and Kolter, R. (2001). Fruiting body formation by *Bacillus subtilis*. Proc. Natl. Acad. Sci. U. S. A. *98*, 11621–11626. https://doi.org/10.1073/pnas.191384198.

Casadaban, M.J., Chou, J., and Cohen, S.N. (1980). In vitro gene fusions that join an enzymatically active B- galactosidase segment to amino-terminal fragments of exogenous proteins: *Escherichia coli* plasmid vectors for the detection and cloning of translational initiation signals. J. Bacteriol. *143*, 971–980. https://doi.org/10.1128/jb.143.2.971-980.1980.

Cazorla, F.M., Romero, D., Pérez-García, A., Lugtenberg, B.J.J., Vicente, A.D., and Bloemberg, G. (2007). Isolation and characterization of antagonistic *Bacillus subtilis* strains from the avocado rhizoplane displaying biocontrol activity. J. Appl. Microbiol. *103*, 1950–1959. https://doi.org/10.1111/j.1365-2672.2007.03433.x.

Chai, Y., Kolter, R., and Losick, R. (2010). An epigenetic switch governing daughter cell separation in *Bacillus subtilis*. Genes Dev. *24*, 754–765. https://doi.org/10.1111/j.1365-2958.2010.07335.x.

Chen, F.Z., You, L.J., Yang, F., Wang, L.N., Guo, X.Q., Gao, F., Hua, C., Tan, C., Fang, L., Shan, R.Q., et al. (2020). CNGBdb: China National GeneBank DataBase. Hereditas *42*, 799–809. https://doi.org/10.16288/j.yczz.20-080.

Chen, Y., Cao, S., Chai, Y., Clardy, J., Kolter, R., Guo, J.H., and Losick, R. (2012). A *Bacillus subtilis* sensor kinase involved in triggering biofilm formation on the roots of tomato plants. Mol. Microbiol. *85*, 418–430. https://doi.org/10.1111/j.1365-2958.2012.08109.x.

Chen, Y., Yan, F., Chai, Y., Liu, H., Kolter, R., Losick, R., and Guo, J.H. (2013). Biocontrol of tomato wilt disease by *Bacillus subtilis* isolates from natural environments depends on conserved genes mediating biofilm formation. Environ. Microbiol. *15*, 848–864. https://doi.org/10.1111/j.1462-2920.2012.02860.x.

Chen, Y., Chen, Y., Shi, C., Huang, Z., Zhang, Y., Li, S., Li, Y., Ye, J., Yu, C., Li, Z., et al. (2018). SOAPnuke: a MapReduce acceleration-supported software for integrated quality control and preprocessing of high-throughput sequencing data. Gigascience *7*, gix120. https://doi.org/10.1093/gigascience/gix120.

Chu, F., Kearns, D.B., Branda, S.S., Kolter, R., and Losick, R. (2006). Targets of the master regulator of biofilm formation in *Bacillus subtilis*. Mol. Microbiol. *59*, 1216–1228. https://doi.org/10.1111/j.1365-2958.2005.05019.x.

Cohn, H.J. (1930). The identity of *Bacillus subtilis*. J. Infect. Dis. *46*, 341–350.

Deatherage, D.E., and Barrick, J.E. (2014). Identification of mutations in laboratory-evolved microbes from Next-Generation Sequencing data using breseq. In Engineering and Analyzing Multicellular Systems. Methods in Molecular Biology (Methods and Protocols), L. Sun and W. Shou, eds. (Humana Press), pp. 165–188. https://doi.org/10.1007/978-1-4939-0554-6_1.

Dragoš, A., Kiesewalter, H., Martin, M., Hsu, C.Y., Hartmann, R., Wechsler, T., Eriksen, C., Brix, S., Drescher, K., Stanley-Wall, N., et al. (2018a). Division of labor during biofilm matrix production. Curr. Biol. *28*, 1903–1913.e5. https://doi.org/10.1016/j.cub.2018.04.046.

Dragoš, A., Lakshmanan, N., Martin, M., Horváth, B., Maróti, G., Falcón García, C., Lieleg, O., and Kovács, Á.T. (2018b). Evolution of exploitative interactions during diversification in *Bacillus subtilis* biofilms. FEMS Microbiol. Ecol. *94*, fix155. https://doi.org/10.1093/femsec/fix155.

Dragoš, A., Martin, M., Falcón García, C., Kricks, L., Pausch, P., Heimerl, T., Bálint, B., Maróti, G., Bange, G., López, D., et al. (2018c). Collapse of genetic division of labour and evolution of autonomy in pellicle biofilms. Nat. Microbiol. *3*, 1451–1460. https://doi.org/10.1038/s41564-018-0263-y.

Egamberdieva, D., Kamilova, F., Validov, S., Gafurova, L., Kucharova, Z., and Lugtenberg, B. (2008). High incidence of plant growth-stimulating bacteria associated with the rhizosphere of wheat grown on salinated soil in Uzbekistan. Environ. Microbiol. *10*, 1–9. https://doi.org/10.1111/j.1462-2920.2007.01424.x.

Elena, S.F., and Lenski, R.E. (2003). Evolution experiments with microorganisms: the dynamics and genetic bases of adaptation. Nat. Rev. Genet. *4*, 457–469. https://doi.org/10.1038/nrg1088.

Endler, A., and Persson, S. (2011). Cellulose synthases and synthesis in *Arabidopsis*. Mol. Plant *4*, 199–211. https://doi.org/10.1093/mp/ssq079.

Fall, R., Kinsinger, R.F., and Wheeler, K.A. (2004). A simple method to isolate biofilm-forming *Bacillus subtilis* and related species from plant roots. Syst. Appl. Microbiol. *27*, 372–379. https://doi.org/10.1078/0723-2020-00267.

Fira, D., Dimkić, I., Berić, T., Lozo, J., and Stanković, S. (2018). Biological control of plant pathogens by *Bacillus* species. J. Biotechnol. *285*, 44–55. https://doi.org/10.1016/j.jbiotec.2018.07.044.

Fujita, M., González-Pastor, J.E., and Losick, R. (2005). High- and low-threshold genes in the Spo0A regulon of *Bacillus subtilis*. J. Bacteriol. *187*, 1357–1368. https://doi.org/10.1128/JB.187.4.1357-1368.2005.

Gallegos-Monterrosa, R., Christensen, M.N., Barchewitz, T., Koppenhöfer, S., Priyadarshini, B., Bálint, B., Maróti, G., Kempen, P.J., Dragoš, A., and Kovács, Á.T. (2021). Impact of Rap-Phr system abundance on adaptation of *Bacillus subtilis*. Commun. Biol. *4*, 468. https://doi.org/10.1038/s42003-021-01983-9.

Gallegos-Monterrosa, R., Mhatre, E., and Kovács, Á.T. (2016). Specific *Bacillus subtilis* 168 variants form biofilms on nutrient-rich medium. Microbiology (United Kingdom) *162*, 1922–1932. https://doi.org/10.1099/mic.0.000371.

Gao, S., Wu, H., Yu, X., Qian, L., and Gao, X. (2016). Swarming motility plays the major role in migration during tomato root colonization by *Bacillus subtilis* SWR01. Biol. Control *98*, 11–17. https://doi.org/10.1016/j.biocontrol.2016.03.011.

Guo, X., Chen, F., Gao, F., Li, L., Liu, K., You, L., Hua, C., Yang, F., Liu, W., Peng, C., et al. (2020). CNSA: a data repository for archiving omics data. Database *2020*, baaa055. https://doi.org/10.1093/database/baaa055.

Guttenplan, S.B., Shaw, S., and Kearns, D.B. (2013). The cell biology of peritrichous flagella in *Bacillus subtilis*. Mol. Microbiol. *87*, 211–229. https://doi.org/10.1111/mmi.12103.

Hassani, M.A., Durán, P., and Hacquard, S. (2018). Microbial interactions within the plant holobiont. Microbiome *6*, 58. https://doi.org/10.1007/978-1-4419-9863-7_100630.

Huang, Y., Wu, Z., He, Y., Ye, B.C., and Li, C. (2017). Rhizospheric *Bacillus subtilis* exhibits biocontrol effect against *Rhizoctonia solani* in Pepper (*Capsicum annuum*). Biomed. Res. Int. *2017*, 1–9. https://doi.org/10.1155/2017/9397619.

Jiang, M., Shao, W., Perego, M., and Hoch, J.A. (2000). Multiple histidine kinases regulate entry into stationary phase and sporulation in *Bacillus subtilis*. Mol. Microbiol. *38*, 535–542. https://doi.org/10.1046/j.1365-2958.2000.02148.x.

Jousset, A., Rochat, L., Péchy-Tarr, M., Keel, C., Scheu, S., and Bonkowski, M. (2009). Predators promote defence of rhizosphere bacterial populations by selective feeding on non-toxic cheaters. ISME J. *3*, 666–674. https://doi.org/10.1038/ismej.2009.26.

Kawecki, T.J., Lenski, R.E., Ebert, D., Hollis, B., Olivieri, I., and Whitlock, M.C. (2012). Experimental evolution. Trends Ecol. Evol. *27*, 547–560. https://doi.org/10.1016/j.tree.2012.06.001.

Kearns, D.B. (2010). A field guide to bacterial swarming motility. Nat. Rev. Microbiol. *8*, 634–644. https://doi.org/10.1038/nrmicro2405.

Kearns, D.B., Chu, F., Branda, S.S., Kolter, R., and Losick, R. (2005). A master regulator for biofilm formation by *Bacillus subtilis*. Mol. Microbiol. *55*, 739–749. https://doi.org/10.1111/j.1365-2958.2004.04440.x.

Kiesewalter, H.T., Lozano-Andrade, C.N., Wibowo, M., Strube, M.L., Maróti, G., Snyder, D., Jørgensen, T.S., Larsen, T.O., Cooper, V.S., Weber, T., and Kovács, Á.T. (2021). Genomic and chemical diversity of *Bacillus subtilis* secondary metabolites against plant pathogenic fungi. mSystems *6*, e00770-20. https://doi.org/10.1101/2020.08.05.238063.

Köhl, J., Kolnaar, R., and Ravensberg, W.J. (2019). Mode of action of microbial biological control agents against plant diseases: relevance beyond efficacy. Front. Plant Sci. *10*, 1–19. https://doi.org/10.3389/fpls.2019.00845.

Konkol, M.A., Blair, K.M., and Kearns, D.B. (2013). Plasmid-encoded ComI inhibits competence in the ancestral 3610 strain of *Bacillus subtilis*. J. Bacteriol. *195*, 4085–4093. https://doi.org/10.1128/JB.00696-13.

Lazarevic, V., Soldo, B., Médico, N., Pooley, H., Bron, S., and Karamata, D. (2005). *Bacillus subtilis* alpha-phosphoglucomutase is required for normal cell morphology and biofilm formation. Appl. Environ. Microbiol. *71*, 39–45. https://doi.org/10.1128/AEM.71.1.39-45.2005.

Lenski, R.E. (2017). What is adaptation by natural selection? Perspectives of an experimental microbiologist. PLoS Genet. *13*, e1006668. https://doi.org/10.1371/journal.pgen.1006668.

Li, E., de Jonge, R., Liu, C., Jiang, H., Friman, V.P., Pieterse, C.M.J., and Bakker, P.A.H.M. (2021a). Rapid evolution of bacterial mutualism in the plant rhizosphere. Nat. Commun. *12*, 3829. https://doi.org/10.2139/ssrn.3650572.

Li, E., Zhang, H., Jiang, H., Pieterse, C.M.J., Jousset, A., Bakker, P.A.H.M., and de Jonge, R. (2021b). Experimental-evolution-driven identification of *Arabidopsis* rhizosphere competence genes in *Pseudomonas protegens*. mBio *12*, e00927-21. https://doi.org/10.1128/mbio.00927-21.

Liebeton, K., Lengefeld, J., and Eck, J. (2014). The nucleotide composition of the spacer sequence influences the expression yield of heterologously expressed genes in *Bacillus subtilis*. J. Biotechnol. *191*, 214–220. https://doi.org/10.1016/j.jbiotec.2014.06.027.

Liepman, A.H., Wightman, R., Geshi, N., Turner, S.R., and Scheller, H.V. (2010). Arabidopsis - a powerful model system for plant cell wall research. Plant J. *61*, 1107–1121. https://doi.org/10.1111/j.1365-313X.2010.04161.x.

Lin, Y., Alstrup, M., Pang, J.K.Y., Maróti, G., Er-Rafik, M., Tourasse, N., Økstad, O.A., and Kovács, Á.T. (2021). Adaptation of *Bacillus thuringiensis* to plant colonization affects differentiation and toxicity. mSystems *6*, e00864-21. https://doi.org/10.1128/msystems.00864-21.

Lozano-Andrade, C.N., Strube, M.L., and Kovács, Á.T. (2021). Complete genome sequences of four soil-derived isolates for studying synthetic microbial community assembly. Microbiol. Resour. Announc. *10*, e00848-21.

Lugtenberg, B., and Kamilova, F. (2009). Plant-growth-promoting rhizobacteria. Annu. Rev. Microbiol. *63*, 541–556. https://doi.org/10.1146/annurev.micro.62.081307.162918.

Martin, M., Dragoš, A., Otto, S.B., Schäfer, D., Brix, S., Maróti, G., and Kovács, Á.T. (2020). Cheaters shape the evolution of phenotypic heterogeneity in *Bacillus subtilis* biofilms. ISME J. *14*, 2302–2312. https://doi.org/10.1038/s41396-020-0685-4.

Mendes, R., Kruijt, M., De Bruijn, I., Dekkers, E., Van Der Voort, M., Schneider, J.H.M., Piceno, Y.M., DeSantis, T.Z., Andersen, G.L., Bakker, P.A.H.M., and Raaijmakers, J.M. (2011). Deciphering the rhizosphere microbiome for disease-suppressive bacteria. Science *332*, 1097–1100. https://doi.org/10.1126/science.1203980.

Mhatre, E., Sundaram, A., Hölscher, T., Mühlstädt, M., Bossert, J., and Kovács, Á. (2017). Presence of calcium lowers the expansion of *Bacillus subtilis* colony biofilms. Microorganisms *5*, 7. https://doi.org/10.3390/microorganisms5010007.

Molina-Santiago, C., Pearson, J.R., Navarro, Y., Berlanga-Clavero, M.V., Caraballo-Rodriguez, A.M., Petras, D., García-Martín, M.L., Lamon, G., Haberstein, B., Cazorla, F.M., et al. (2019). The extracellular matrix protects *Bacillus subtilis* colonies from *Pseudomonas* invasion and modulates plant co-colonization. Nat. Commun. *10*, 1919. https://doi.org/10.1038/s41467-019-09944-x.

Nordgaard, M., Mortensen, R.M.R., Kirk, N.K., Gallegos-Monterrosa, R., and Kovács, Á.T. (2021). Deletion of Rap-Phr systems in *Bacillus subtilis* influences in vitro biofilm formation and plant root colonization. Microbiologyopen *10*, e1212. https://doi.org/10.1002/mbo3.1212.

Ongena, M., and Jacques, P. (2008). *Bacillus* lipopeptides: versatile weapons for plant disease biocontrol. Trends Microbiol. *16*, 115–125. https://doi.org/10.1016/j.tim.2007.12.009.

Pandey, A., and Palni, L.M.S. (1997). *Bacillus* species: the dominant bacteria of the rhizosphere of established tea bushes. Microbiol. Res. *152*, 359–365. https://doi.org/10.1016/S0944-5013(97)80052-3.

Poltak, S.R., and Cooper, V.S. (2011). Ecological succession in long-term experimentally evolved biofilms produces synergistic communities. ISME J. *5*, 369–378. https://doi.org/10.1038/ismej.2010.136.

Reverdy, A., Chen, Y., Hunter, E., Gozzi, K., and Chai, Y. (2018). Protein lysine acetylation plays a regulatory role in *Bacillus subtilis* multicellularity. PLoS One *13*, e0204687. https://doi.org/10.1371/journal.pone.0204687.

Richter, A., Hölscher, T., Pausch, P., Sehrt, T., Brockhaus, F., Bange, G., and Kovács, Á.T. (2018). Hampered motility promotes the evolution of wrinkly phenotype in *Bacillus subtilis*. BMC Evol. Biol. *18*, 155. https://doi.org/10.1186/s12862-018-1266-2.

Ross-Gillespie, A., Gardner, A., West, S.A., and Griffin, A.S. (2007). Frequency dependence and cooperation: theory and a test with bacteria. Am. Nat. *170*, 331–342. https://doi.org/10.1086/519860.

Rudrappa, T., Czymmek, K.J., Paré, P.W., and Bais, H.P. (2008). Root-secreted malic acid recruits beneficial soil bacteria. Plant Physiol. *148*, 1547–1556. https://doi.org/10.1104/pp.108.127613.

Schindelin, J., Arganda-Carreras, I., Frise, E., Kaynig, V., Longair, M., Pietzsch, T., Preibisch, S., Rueden, C., Saalfeld, S., Schmid, B., et al. (2012). Fiji: an open-source platform for biological-image analysis. Nat. Methods *9*, 676–682. https://doi.org/10.1038/nmeth.2019.

Sprouffske, K., and Wagner, A. (2016). Growthcurver: an R package for obtaining interpretable metrics from microbial growth curves. BMC Bioinformatics *17*, 172. https://doi.org/10.1186/s12859-016-1016-7.

Subramaniam, A.R., Deloughery, A., Bradshaw, N., Chen, Y., O'Shea, E., Losick, R., and Chai, Y. (2013). A serine sensor for multicellularity in a bacterium. Elife *2*, e01501. https://doi.org/10.7554/eLife.01501.

Thérien, M., Kiesewalter, H.T., Auria, E., Charron-Lamoureux, V., Wibowo, M., Maróti, G., Kovács, Á.T., and Beauregard, P.B. (2020). Surfactin production is not essential for pellicle and root-associated biofilm development of *Bacillus subtilis*. Biofilm *2*, 100021. https://doi.org/10.1016/j.bioflm.2020.100021.

Tian, T., Sun, B., Shi, H., Gao, T., He, Y., Li, Y., Liu, Y., Li, X., Zhang, L., Li, S., et al. (2021). Sucrose triggers a novel signaling cascade promoting *Bacillus subtilis* rhizosphere colonization. ISME J. *15*, 2723–2737. https://doi.org/10.1038/s41396-021-00966-2.

Trivedi, P., Leach, J.E., Tringe, S.G., Sa, T., and Singh, B.K. (2020). Plant–microbiome interactions: from community assembly to plant health. Nat. Rev. Microbiol. *18*, 607–621. https://doi.org/10.1038/s41579-020-0412-1.

van den Bergh, B., Swings, T., Fauvart, M., and Michiels, J. (2018). Experimental design, population dynamics, and diversity in microbial experimental evolution. Microbiol. Mol. Biol. Rev. *82*. e00008-18. https://doi.org/10.1128/mmbr.00008-18.

van Ditmarsch, D., Boyle, K.E., Sakhtah, H., Oyler, J.E., Nadell, C.D., Déziel, É., Dietrich, L.E.P., and Xavier, J.B. (2013). Convergent evolution of hyperswarming leads to impaired biofilm formation in pathogenic bacteria. Cell Rep. *4*, 697–708. https://doi.org/10.1016/j.celrep.2013.07.026.

van Gestel, J., Weissing, F.J., Kuipers, O.P., and Kovács, Á.T. (2014). Density of founder cells affects spatial pattern formation and cooperation in *Bacillus subtilis* biofilms. ISME J. *8*, 2069–2079. https://doi.org/10.1038/ismej.2014.52.

Varon, D., Boylan, S.A., Okamoto, K., and Price, C.W. (1993). *Bacillus subtilis gtaB* encodes UDP-glucose pyrophosphorylase and is controlled by stationary-phase transcription factor σB. J. Bacteriol. *175*, 3964–3971. https://doi.org/10.1128/jb.175.13.3964-3971.1993.

Vlamakis, H., Aguilar, C., Losick, R., and Kolter, R. (2008). Control of cell fate by the formation of an architecturally complex bacterial community. Genes Dev. *22*, 945–953. https://doi.org/10.1101/gad.1645008.4.

Xu, Z., Zhang, H., Sun, X., Liu, Y., Yan, W., Xun, W., Shen, Q., and Zhang, R. (2019). *Bacillus velezensis* wall teichoic acids are required for biofilm formation and root colonization. Appl. Environ. Microbiol. *85*, e02116–e02118. https://doi.org/10.1128/aem.02116-18.

Zeigler, D.R., Prágai, Z., Rodriguez, S., Chevreux, B., Muffler, A., Albert, T., Bai, R., Wyss, M., and Perkins, J.B. (2008). The origins of 168, W23, and other *Bacillus subtilis* legacy strains. J. Bacteriol. *190*, 6983–6995. https://doi.org/10.1128/JB.00722-08.

Zhu, B., and Stülke, J. (2018). SubtiWiki in 2018: from genes and proteins to functional network annotation of the model organism *Bacillus subtilis*. Nucleic Acids Res. *46*, D743–D748. https://doi.org/10.1093/nar/gkx908.

STAR★METHODS

KEY RESOURCES TABLE

REAGENT or RESOURCE	SOURCE	IDENTIFIER
Chemicals, peptides, and recombinant proteins		
Lysogeny Broth (LB)	Carl Roth GmbH	Catalog # X964.2
Tryptic Soy Broth (TSB)	Sigma-Aldrich	Catalog # 22098-500G-F
Agar	Carl Roth GmbH	Catalog # 5210.2
Potassium Hydrogen Phosphate	Carl Roth GmbH	Catalog # P749.2
Potassium Dihydrogen Phosphate	Carl Roth GmbH	Catalog # 3904.1
MOPS	Carl Roth GmbH	Catalog # 6979.3
Magnesium chloride hexahydrate	Carl Roth GmbH	Catalog # 2189.1
Manganese(II) chloride	Carl Roth GmbH	Catalog # T881.3
Zinc chloride	Carl Roth GmbH	Catalog # T887.1
Thiamine	Carl Roth GmbH	Catalog # T911.1
Calcium chloride	Carl Roth GmbH	Catalog # 5239.1
Ammonium chloride	Carl Roth GmbH	Catalog # K298.2
Glycerol	Carl Roth GmbH	Catalog # 7533.1
Cellobiose	Carl Roth GmbH	Catalog # 5840.3
Xylan from beechwood	Carl Roth GmbH	Catalog # 4414.3
Starch from potatoes	Carl Roth GmbH	Catalog # 9441.1
Potassium hydroxide	Carl Roth GmbH	Catalog # 6751.1
Sodium hypochlorite	VWR	Catalog # 27900.296
Murashige and Skoog basal salts mixture	Sigma-Aldrich	Catalog # M5519
Spectinomycin dihydrochloride	VWR	J61820.14
Experimental models: Organisms/strains		
DK1042: *B. subtilis* NCIB 3610 *comI*^{Q12I}	(Konkol et al., 2013)	Strain DK1042
TB500.1: DK1042 *amyE*::$P_{hyperspank}$-*gfp* Spec^R	(Mhatre et al., 2017)	N/A
TB501.1: DK1042 *amyE*::$P_{hyperspank}$-*mKATE2* Spec^R	(Dragoš et al., 2018a)	N/A
TB530.1: DK1042 *amyE*::$P_{hyperspank}$-*gfp* Spec^R *hag*::Km^R		N/A
TB531.1: DK1042 *amyE*::$P_{hyperspank}$-*mKATE2* Spec^R *hag*::Km^R		N/A
DTUB310: DK1042 Ev6.1 *amyE*::$P_{hyperspank}$-*gfp* Spec^R	This study	N/A
DTUB311: DK1042 Ev6.1 *amyE*::$P_{hyperspank}$-*mKATE2* Spec^R		
DTUB312: DK1042 Ev7.3 *amyE*::$P_{hyperspank}$-*gfp* Spec^R		
DTUB313: DK1042 Ev7.3 *amyE*::$P_{hyperspank}$-*mKATE2* Spec^R		
D749: *Pedobacter* sp	(Lozano-Andrade et al., 2021)	N/A
D757: *Rhodococcus globerulus*		N/A
D763: *Stenotrophomas indicatrix*		N/A
D764: *Chryseobacterium* sp		N/A
MC1061: *Escherichia coli* K-12 F λ Δ(*ara-leu*)*7697* [*araD139*]$_{B/r}$ Δ(*codB-lacI*)*3 galK16 galE15* e14 *mcrA0 relA1 rpsL150*(Str^R) *spoT1 mcrB1 hsdR2*(r m$^+$)	(Casadaban et al., 1980)	N/A
Arabidopsis thaliana Col-0	NASC	N/A
Recombinant DNA		
pTB497.1	(van Gestel et al., 2014)	N/A
pTB498.1	(Dragoš et al., 2018b)	N/A

(*Continued on next page*)

Continued

REAGENT or RESOURCE	SOURCE	IDENTIFIER
Software and algorithms		
Zen 3.1 Software	Carl Zeiss, Oberkochen, Germany	https://www.zeiss.com/corporate/int/home.html
ImageJ	(Schindelin et al., 2012)	https://imagej.nih.gov/ij/
OriginPro 2020	OriginLab, Northampton, MA, USA	https://www.originlab.com/
R Studio	RStudio, Boston, MA, USA	https://www.rstudio.com/
bcl2fastq (v2.17.1.14)	Illumina, San Diego, CA, USA	https://www.illumina.com/
CLC Genomics Workbench	Qiagen, Hilden, Germany	https://digitalinsights.qiagen.com
SOAPnuke (v1.5.6)	(Chen et al., 2018)	https://github.com/BGI-flexlab/SOAPnuke
breseq (v0.35.7)	(Deatherage and Barrick, 2014)	https://barricklab.org/twiki/bin/view/Lab/ToolsBacterialGenomeResequencing
Others		
Glass beads Ø0.25-0.5 mm,	Carl Roth GmbH	Catalog # A553.1

RESOURCE AVAILABILITY

Lead contact

Further information and requests for resources and reagents should be directed to and will be fulfilled by the Lead Contact, Ákos T. Kovács (atkovacs@dtu.dk).

Materials availability

Bacterial isolates derived from the experimental evolution in this study are available upon request from Ákos T. Kovács (atkovacs@dtu.dk). This study did not generate new unique plasmids or reagents.

Data and code availability

The sequencing data for single evolved isolates has been deposited into the NCBI Sequence Read Archive (SRA) database under BioProject accession number: PRJNA705352, and sequencing data for endpoint populations into CNGB Sequence Archive (CNSA) (Guo et al., 2020) of China National GeneBank DataBase (CNGBdb) (Chen et al., 2020) with accession number CNP0002416.

Other data reported in this study is available from the lead contact upon reasonable request.

This study does not report any new, original code.

Any Additional information can be obtained upon request from Ákos T. Kovács (atkovacs@dtu.dk).

EXPERIMENTAL MODEL AND SUBJECT DETAILS

Bacterial strains and culture media

Bacillus subtilis DK1042 strain, an easily transformable derivative of the undomesticated *B. subtilis* NCBI 3610 (Konkol et al., 2013), was used as ancestor for the experimental evolution. For pairwise competitions between the ancestor and evolved isolates, and for root co-colonization with a synthetic, soil-derived community, TB500.1 and TB501.1, that were previously created by transforming DK1042 with pTB497.1 and pTB498.1 (Dragoš et al., 2018a; Mhatre et al., 2017), respectively, were used as the ancestor. In addition, selected evolved isolates derived from the ancestor were transformed with plasmids pTB497.1 and pTB498.1. These plasmids harbor the *gfp* and *mKATE* gene, respectively, under the control of the hyper-spank (constitutive) promoter and a spectinomycin resistance gene within the flanking regions of the *amyE* gene. Transformants were identified by selecting for spectinomycin resistance and double cross-overs were verified by the loss of amylase activity on LB agar + starch plates.

The four bacterial species, *Pedobacter* sp., *Rhodococcus globerulus*, *Stenotrophomas indicatrix* and *Chryseobacterium* sp., constituting a synthetic, soil-derived community were previously acquired in

Dyrehaven, Kongens Lyngby, Denmark (55° 47′ 19.68″ N, 12° 33′ 29.88″ E), as described (Lozano-Andrade et al., 2021). An overview of the strains used in this study is included in the Key Resources Table.

B. subtilis strains were routinely grown overnight (ON) in Lysogeny Broth (LB; LB-Lennox, Carl Roth, Germany; 10 g/L tryptone, 5 g/L yeast extract and 5 g/L NaCl) at 37°C while shaking at 220 rpm. When relevant, spectinomycin was added at a final concentration of 100 μg/mL. The bacterial species used for the synthetic, soil-derived community were grown for 48 h in 0.1% (w/v) Tryptic Soy Broth (TSB; Sigma-Aldrich, St. Louis, Missouri, USA) at room temperature. For the experimental evolution on plant roots and root colonization assays, a minimal salts nitrogen glycerol (MSNg) medium was used. MSNg was prepared as follows: The base was prepared by adding 0.026 g KH_2PO_4, 0.061 g K_2HPO_4, 2.09 g MOPS and 0.04 g $MgCl_2$ x $6H_2O$ per 100 mL dH_2O and adjusting the pH to 7.0 using KOH. The base was autoclaved, cooled down to room temperature and then supplemented with 0.05 mL of 100 mM $MnCl_2$, 0.1 mL of 1 mM $ZnCl_2$, 0.1 mL of 2 mM thiamine, 0.1 mL of 0.7 M $CaCl_2$, NH_4Cl_2 to a final 0.2% and glycerol to a final 0.05%. Growth of *B. subtilis* ancestor and evolved isolates alone or in co-culture with the synthetic, soil-derived community was monitored in MSNc + xylan, which was prepared similarly to MSNg except that instead of glycerol, cellobiose and xylan were added to a final concentration of 0.5%. Pellicle biofilm formation was assessed in LB medium with or without a supplementation of xylan (0.5%) (w/v). Pairwise competitions between the ancestor and evolved isolates were evaluated in LB + xylan (0.5%).

Plant material

Arabidopsis thaliana Col-0 seedings were used as plant host for the experimental evolution and root colonization assays. The seeds were surface sterilized in a 2% (v/v) sodium hypochlorite solution (VWR, Radnor, Pennsylvania, USA) and shaken on an orbital mixer for 12 minutes. The seeds were washed five times in sterile, distilled water. Approximately 15 sterilized seeds were carefully pipetted onto pre-dried MS agar plates (Murashige and Skoog basal salts mixture, Sigma-Aldrich) (2.2 g L^{-1}, pH = 5.6–5.8 supplemented with 1% agar). Plates were sealed with parafilm and stratified at 4°C for 3 days, and were then placed at an angle of 65°C in a plant chamber (cycles of 16 h light at 24°C, and 8 h dark at 20°C). The seedlings were grown in the plant chamber for 6-8 days before use.

METHOD DETAILS

Experimental evolution of *B. subtilis* on *A. thaliana* seedlings

To study the evolutionary adaptation of *B. subtilis* to *A. thaliana* roots, we employed an experimental evolution (EE) setup similar to the one established by Lin et al. (2021). This setup was inspired by a long-term EE on polystyrene beads (Poltak and Cooper, 2011), but instead of beads, *A. thaliana* roots were used for successive root colonization by *B. subtilis*. The EE on plant seedlings was carried out under axenic, hydroponic conditions optimized for *B. subtilis* (Beauregard et al., 2013; Dragoš et al., 2018a; Gallegos-Monterrosa et al., 2016; Nordgaard et al., 2021; Thérien et al., 2020). Seven parallel populations were initiated by inoculating *A. thaliana* seedlings, placed in 300 μL MSNg medium in 48-well plates, with *B. subtilis* DK1042 at a starting OD_{600} of 0.02. In addition, a replicate with a sterile root in MSNg without bacterial inoculation was included as a control. The 48-well plate was incubated in a plant chamber (cycles of 16 h light at 24°C/8 h dark at 20°C) at mild agitation (90 rpm). After 48 h, the colonized seedling was washed twice in MSNg and transferred to fresh medium containing a new, sterile seedling enabling re-colonization. Following this approach, the seven parallel populations were serially transferred every 48 h for a total of 32 transfers. At different time points during the ongoing EE, the old seedlings were washed twice in MSNg and vortexed with glass beads to disperse the biofilm. The resulting cell suspension was used for plating to follow the productivity of the evolving populations, i.e. colony-forming unit (CFU) per root, and also preserved as frozen (−80°C) stocks for later analysis.

Isolation of single evolved isolates and colony morphology assay

Frozen stocks of population 3, 4, 6 and 7 from three different time points during the EE (transfer 12, 18 and 30) were streaked on LB plates to obtain single colonies of evolved isolates. Transfer 30 (T30) was designated as the final transfer for the isolation of evolved isolates. From each population and time point, three colonies were randomly selected, prepared as ON cultures and saved as frozen stocks. Colony morphologies of evolved isolates were examined by spotting 2 μL ON cultures on LB agar (1.5%) and incubated at 30°C for 48 h. Importantly, by growing the ancestor and evolved isolates from frozen stocks in LB ON,

all isolates should be in a similar physiological state, so a potential difference in colony morphology should be attributed to genetic variation.

Root colonization assay

The evolved isolates were tested for root colonization under the same conditions applied during the EE. For individual root colonization, sterile *A. thaliana* seedlings in MSNg medium were inoculated with the ancestor or evolved isolates at a starting OD_{600} of 0.02. For pairwise competition experiments, sterile *A. thaliana* seedlings were inoculated with a 1:1 mix of the ancestor and evolved isolates with opposite, fluorescent labels. Importantly, to obtain a similar starting cell number for the competition experiment, ON cultures of the ancestor and isolate Ev6.1 were adjusted to an OD_{600} of 0.2, while Ev7.3 was adjusted to an OD_{600} of 1.0 corresponding to comparable total cell counts. For plant co-colonization by *B. subtilis* in the presence of a soil-derived synthetic community, cell suspensions of *Pedobacter* sp. D749 and *Rhodococcus globerulus* D757 were adjusted to an OD_{600} of 2.0, *Stenotrophomas indicatrix* D763 to an OD_{600} of 0.05 and *Chryseobacterium* sp. D764 to an OD_{600} of 0.1 and mixed by equal volumes (hereafter referred to as community). This mix was further adjusted to an OD_{600} of 0.2. OD-adjusted *B. subtilis* ancestor (OD_{600} of 0.2) or Ev7.3 (OD_{600} of 1.0) and community were co-inoculated in four different ratios (0.1:1, 1:1, 10:1, 100:1 of *B. subtilis* and community, respectively) into MSNg medium containing a sterile *A. thaliana* seedling. The 48-well plates of all root colonization assays were incubated in the plant chamber at mild agitation (90 rpm). After 48 h, the colonized seedling was washed twice in MSNg and either vortexed with glass beads, and the resulting cell suspension plated for CFU quantification, or transferred to a glass slide for imaging using confocal laser scanning microscopy (CLSM).

For root colonization competition between *B. subtilis* WT and the Δ*hag* mutant, ON cultures of the WT and Δ*hag* mutant with opposite fluorescent labels were mixed 1:1 and inoculated onto sterile *A. thaliana* seedlings in MSNg medium at a starting OD_{600} of 0.02. Plates were incubated in the plant chamber under static or shaking conditions (200 rpm) for 48 h. The seedlings were then washed in MSNg and transferred to fresh medium containing a new, sterile seedling and incubated under the same conditions as before (i.e. static or shaking conditions). This step was repeated once more, after which the third root was washed and vortexed with glass beads, and the resulting cell suspension was plated for CFU quantification.

Pairwise competition experiments in LB + xylan

ON cultures of the ancestor and selected evolved isolates were adjusted to an OD_{600} of 5.0. Ancestor was mixed 1:1 and 1:5 by volume with Ev6.1 and Ev7.3, respectively, to obtain a comparable number of starting cells. 80 μL of the mix was inoculated into 20 mL LB + xylan (0.5%) medium in 100 mL bottles, giving a starting OD_{600} of 0.02. Bottles were incubated at 37°C while shaking at 220 rpm for 48 h followed by plating for CFU quantification.

Biofilm formation in response to plant polysaccharides

To test for pellicle biofilm formation in response to plant polysaccharides, the ancestor or the evolved isolates were inoculated into 1.5 mL LB + xylan (0.5%) medium in 24-well plates to a starting OD_{600} of 0.05 and incubated under static conditions at 30°C for 48 h. In addition, the ancestor and evolved isolates were evaluated for biofilm formation in LB without supplementation.

Motility assays

Swimming motility was tested using soft agar plates (15 mL LB with 0.3% agar) dried for 5 minutes while swarming motility was evaluated on semi-soft agar plates (15 mL LB with 0.7% agar) dried for 20 minutes. 2 μL ON cultures of the ancestor or evolved isolates adjusted to an OD_{600} of 0.5 were spotted in the middle of a petri dish and incubated at 37°C. Multiple stacking was avoided in order to keep a similar humidity across all plates. Swimming and swarming motility were followed for 6 and 8 h, respectively. For each plate, motility was quantified as the averaged radius measured in four different directions.

Growth in the presence of xylan

To monitor the growth of ancestor and evolved isolates in the presence of plant compounds, two independent ON cultures of each isolate were independently inoculated into a 96-well plate containing 100 μL MSNc + xylan (0.5%) medium at a starting OD_{600} of 0.1. OD_{600} was monitored in a plate reader (BioTek Synergy HTX Multi-Mode Microplate Reader) every 15 min for 55 h at 24°C under continuous shaking (orbital).

To test for growth in co-culture with the community, two to three independent ON cultures of constitutively GFP-labelled *B. subtilis* ancestor and Ev7.3 were adjusted to an OD_{600} of 0.1 in MSNc + xylan (0.5%). Cell suspensions of the four community members were adjusted in MSNc + xylan (0.5%) to the same OD_{600} values used for the root colonization assay (see above), and the mixed community was adjusted to a final OD_{600} of 0.1. Ancestor or Ev7.3 was co-inoculated with the community in the same ratios as for the root colonization assay (0.1:1, 1:1, 10:1 and 100:1 of *B. subtilis* and community, respectively). OD_{600} and GFP were monitored in the plate reader every 15 minutes for 35 h at 24°C under continuous shaking (orbital). In both growth assays, each well was measured at 9 (OD_{600}) or 5 ($GFP_{485/20nm}$) different points to avoid artifacts due to aggregation.

Pairwise interactions of *B. subtilis* with community members

To study potential altered interactions with any of the four bacterial species of the community, 2 μL of ON cultures of *B. subtilis* ancestor or Ev7.3 adjusted to an OD_{600} of 0.5 was spotted on LB agar (1.5%). On the same plate, 2 μL of cell suspensions of *Pedobacter* sp. (OD_{600} of 2.0), *Rhodococcus globerulus* (OD_{600} of 2.0), *Stenotrophomas indicatrix* (OD_{600} of 0.1) or *Chryseobacterium* sp. (OD_{600} of 0.1) were spotted at a 0.7 cm distance from the *B. subtilis* inoculum. The plates were incubated at 30°C.

Microscopy/confocal laser scanning microscopy (CLSM)

Bright-field images of colonies, whole pellicle biofilms and pairwise interactions were acquired with an Axio Zoom V16 stereomicroscope (Carl Zeiss, Germany) equipped with a Zeiss CL 9000 LED light source and an AxioCam MRm monochrome camera (Carl Zeiss, Germany). Images of colonized seedlings were acquired using CLSM (Leica Microsystems Confocal Microscope SP8, Germany). The seedlings were washed twice in MSNg and placed onto glass slides. Images were obtained using the 63×/1.4 OIL objective. Fluorescent reporter excitation was performed with the argon laser at 488 nm while the emitted fluorescence of GFP and mKate was recorded at 484–536 nm and 567–654 nm, respectively. For each competition, three images from three independent seedlings were obtained. Representative images were used to visualize root colonization. Zen 3.1 Software (Carl Zeiss) and ImageJ was used for image visualization.

Genome re-sequencing and genome analysis of single isolates and endpoint populations

Genomic DNA of selected evolved isolates from different time points and whole populations from the final transfer (T30) of the EE was extracted from 2 mL ON cultures using the EURx Bacterial and Yeast Genomic DNA Kit. Resequencing of single evolved isolates was performed as previously described (Dragoš et al., 2018b, 2018c; Gallegos-Monterrosa et al., 2021; Martin et al., 2020; Thérien et al., 2020). Briefly, paired-end libraries were prepared using the NEBNext® Ultra™ II DNA Library Prep Kit for Illumina. Paired-end fragment reads were generated on an Illumina NextSeq sequencer using TG NextSeq® 500/550 High Output Kit v2 (300 cycles). Primary data analysis (base-calling) was carried out with "bcl2fastq" software (v2.17.1.14, Illumina). All further analysis steps were done in CLC Genomics Workbench. Reads were quality-trimmed using an error probability of 0.05 (Q13) as the threshold. In addition, the first ten bases of each read were removed. Reads that displayed ≥80% similarity to the reference over ≥80% of their read lengths were used in the mapping. Non-specific reads were randomly placed to one of their possible genomic locations. Quality-based SNP and small In/Del variant calling was carried out requiring ≥8 × read coverage with ≥25% variant frequency. Only variants supported by good quality bases (Q ≥ 20) were considered and only when they were supported by evidence from both DNA strands in comparison to the *B. subtilis* NCIB 3610 genome and pBS plasmid (GenBank accession no. NZ_CP020102 and NZ_CP020103, respectively).

For whole-population sequencing of the evolved populations from the final time point, acoustic fragmentation PCR-free libraries were prepared using MGIEasy PCR-free Library Prep Set (MGI Tech). Paired-end fragment reads (150bp x 2) were generated on a DNBSEQ-Tx sequencer (MGI Tech) following the manufacturer's procedures. All population samples were sequenced with >200 x coverage for polymorphism calling. Raw data were filtered using SOAPnuke (v1.5.6) (Chen et al., 2018) to remove low quality reads: reads including more than 50% of bases with quality lower than 12, reads including more than 10% of unknown base "N," and reads containing adaptor contamination. Mutations were called using *Breseq* (v0.35.7) with the default parameters and a -p option for population samples (Deatherage and Barrick, 2014). The default parameters called mutations only if they appeared at least 2 times from each strand and reached a frequency of at least 5% in the population. Similar to single evolved isolates, the *B. subtilis* NCIB 3610 genome and pBS plasmid were used as references for mutation calling. For both

single evolved isolates and whole populations, mutations were removed if they were also found in the ancestor to obtain the final mutation set. Identified mutations in the evolved isolates and whole populations are listed in Tables S1 and S2, respectively.

The sequencing data for single evolved isolates that support the findings of this study has been deposited into the NCBI Sequence Read Archive (SRA) database under BioProject accession number: PRJNA705352, and sequencing data for endpoint populations into CNGB Sequence Archive (CNSA) (Guo et al., 2020) of China National GeneBank DataBase (CNGBdb) (Chen et al., 2020) with accession number CNP0002416.

QUANTIFICATION AND STATISTICAL ANALYSIS

Data and statistical analysis

Data and statistical analysis were carried out in Excel, OriginPro and R Studio. Outliers were identified using Dixon's test for outliers. For all statistical tests, normality was evaluated with a Shapiro-Wilk test. Equal variance was tested using F-test (for two groups) or Levene's test (for more than two groups). In addition, p-values were corrected for multiple testing using the Benjamini & Hochberg (BH) procedure within each series of experiments. For all statistical tests, a significance level of 0.05 was used. No statistical methods were used to pre-estimate sample size and the experiments were not randomized.

For individual root colonization, the log10-transformed productivity (CFU/mm root) of the replicates were divided by the mean of the log10-transformed productivity of the ancestor from the same experimental setup. For competition between WT and the Δ*hag* mutant, the observed frequencies of the WT after 48 h (on the third root) were divided by 0.5 (the starting frequency in the inoculation mix). For these experiments, the resulting normalized values were subjected to a One-sample *t*-test to test whether the mean was significantly different from 1. For pairwise competitions between the ancestor and evolved isolates on the root or in LB + xylan, the relative fitness (r) of the evolved isolate was calculated by comparing the frequency of the evolved isolate at the beginning and the end of the competition experiment as shown in Equation 1 (Jousset et al., 2009; Li et al., 2021a; Ross-Gillespie et al., 2007), in which X_0 is the initial and X_1 is the final frequency of the evolved isolate. The relative fitness was log2-transformed, and these values were subjected to a One-sample *t*-test to test whether the mean was significantly different from 0.

$$\text{Relative fitness } (r) = \frac{X_1(1 - X_0)}{X_0(1 - X_1)} \qquad \text{(Equation 1)}$$

For root co-colonization of the ancestor and Ev7.3 with the community, within each inoculation ratio, statistical significance between *B. subtilis* ancestor and Ev7.3, and between the communities co-inoculated with the ancestor or with Ev7.3 was tested with a Two-sample *t*-test. If the groups had unequal variance, Welch's Two-sample *t*-test was applied.

For swimming and swarming motility, an ANOVA was performed on the log10-transformed data at each time point followed by a Dunnett's Multiple Comparison test using the ancestor as the control group.

For growth curve analysis of the ancestor and evolved isolates in monoculture, the carrying capacity (K) of individual replicates was calculated from the OD_{600} data using the Growthcurver-package in R (Sprouffske and Wagner, 2016). Significant difference in carrying capacity between ancestor and evolved isolates was tested by an ANOVA followed by a Dunnett's Multiple Comparison test. Similarly, for the growth profiles of *B. subtilis* ancestor and Ev7.3 in co-culture with the community, the carrying capacity (K) was calculated from the $GFP_{485/20nm}$ data. Significant difference between ancestor and Ev7.3 under the same inoculation ratio or alone was tested by a Two-sample *t*-test or Wilcoxon Unpaired Two-sample test (when data failed to meet parametric assumptions).